IN-90-CR

321366

THE UNIVERSITY OF MICHIGAN
DEPARTMENT OF ATMOSPHERIC, OCEANIC, AND SPACE SCIENCE

Space Physics Research Laboratory
2245 Hayward Street
Ann Arbor, Michigan 48109-2143

P-55

Contract/Grant No.:	NAGW-1907
Project Name:	Distribution of Gas in the Inner Comae of Comets
Report Author(s):	M. Combi
Author(s) Phone:	313/764-6226
Report Preparation Date:	December 1990
Report Type:	Final Technical Report
Period Covered:	November 89 - October 90
Project Director: **Principal Investigator(s):**	Michael Combi
Program Technical Officer: **Address:**	Jay T. Bergstralh Code EL NASA Headquarters Washington, D.C. 20546

(NASA-CR-187723) DISTRIBUTION OF GAS IN THE INNER COMAE OF COMETS Final Report, Nov. 1989 - Oct. 1990 (Michigan Univ.) 55 p
CSCL 03B

N91-15955

Unclas
G3/90 0321366

I. Introduction

In order to understand the physical and chemical processes which produce the observed spatial morphology of the cometary coma, it is necessary to analyze observational data with physically meaningful models. With this in mind, the goals of this project have been to undertake a coupled program of theoretical modeling and complementary observational data analysis regarding the spatial distributions of neutral gases in the coma. More specifically, the particular topics of interest are: (1) the theoretical modeling of the non-equilibrium dynamics of the inner coma with emphasis on the region of the coma from the transition from collisional fluid flow out to the free-flow region and on observable conditions in the coma (i.e. density, outflow speed, and temperature), and (2) the model analysis of an important set of long-slit CCD spectra of comets.

A range of approaches for modeling the cometary coma have been employed by many investigators. The Monte Carlo and the coupled hydrodynamic/Monte Carlo approaches to modeling the cometary coma recognize that the region of the coma typically observed is that where collisions do occur between molecules, but where not enough collisions occur to be able to describe the coma as a fluid. Furthermore, outside this transition region, the Monte Carlo model have already been demonstrated to be a powerful tool for representing the complexities of free molecular flow, such as time-dependence, radiation pressure, the orbital mechanics of individual particles, etc. The theoretical modeling involves the continued development and use of Monte Carlo models and coupled hydrodynamic/Monte Carlo models for the outflowing cometary coma.

The observational data analysis portion of this project is an integral and important part of the overall picture. Developing sophisticated models is not an end unto itself. The models are only important if they can explain and be tested by observational data. Conversely, models are used for the interpretation and analysis of observational data by necessity. The side-by-side development of models along with the observation and analysis of data is an important and integral part of this project. The understanding of data from Halley is a valuable endeavor for the preparation of NASA's CRAF (Comet Rendezvous Asteroid Flyby) mission. The scientific community has in hand valuable observational and *in situ* data regarding one comet (Halley). It is important to use Halley as the benchmark by which other remotely observed comet data can be understood. The self-consistent analysis of data with appropriate models is therefore of the utmost importance.

The data analysis work for this project includes the analysis of the spatial profiles of [OI], NH_2, CN and C_2. It is being carried out in collaboration with Dr. Uwe Fink of the University of Arizona who with his co-workers observed comet Halley extensively during both the pre and post perihelion periods.

II. Progress during this Year

Significant progress was made this year in both the theoretical and the observational data analysis areas. Each area will be discussed separately.

II.A. Theoretical Modeling

In a collisional Monte Carlo model for the cometary coma, the trajectories of molecules are calculated explicitly, following the the complete time history of the particle from its production at the nucleus through various stages of photodissociation, entrainment within the outflowing coma, and/or inter-molecular collisions. Between two collisions, the path length of a particle is calculated given a set of random numbers and a mathematical description of the conditions regarding the state of the background gas through which it moves. These conditions are the temperature and bulk motion of the gas. Two special cases of the collision path length were presented in the paper by Combi and Smyth (1988a). One was for the important limit which is correct for the fast moving H atoms and yields a collision path integral which is integrable and therefore fast to compute in a model. It essentially assumes that the coma is stationary and has negligible temperature. The other case was the more general one which accounted for the relative motion of the particle with respect to the outflowing coma, but where the coma temperature was still neglected. It should be noted here that for the purpose of computing gas density (or similarly the resulting column density) profiles, the simpler formulations of Combi and Smyth (1988a) are quite adequate.

On the other hand if one is interested in information about the velocity distribution function, then neither of these formulations treats nearly thermalized heavy molecules very well. Therefore, we have performed the derivation of the more general case of the collision rate at any location in a radially outflowing coma with a given Maxwell-Boltzmann temperature. It has been incorporated it into the model. The collision rate for a particle in the coma at a distance r_o from the center of the nucleus of the comet is obtained by integrating the relative velocity weighted velocity distribution function over the three-space velocity. It is given by

$$\upsilon = \frac{Q\sigma U}{4\pi r_o^2 c_o}\left[erf(U\sqrt{\alpha})\left\{1+\frac{1}{2U^2\alpha}\right\}+\frac{exp(-U^2\alpha)}{\sqrt{\pi\alpha}U}\right]$$

where

$$U = (u^2 - 2uc_o \cos\theta + c_o^2)^{1/2}$$

$$\beta = c_o / u$$

$$\alpha = m / 2kT$$

c_O = coma outflow speed

u = particle speed

θ = particle direction angle relative to the outward radial

σ = collision cross section between the particle and the coma gas

Q = coma gas production rate.

In the Monte Carlo model a random number on the interval from 0 to 1 is set equal to the collision probability along the path and the collision path length corresponding to that random number is then chosen. Since the outflow speed and temperature vary significantly only for large changes in radial distance, we can assume (as in Combi and Smyth 1988a) that over any one collision path they are both constant. This calculation results in the following integral equation:

$$-ln(1 - R_i) = \frac{Q\sigma}{4\pi c_o r_o \gamma} \int_0^{\lambda} \frac{v_{\lambda'}[erf(v_{\lambda'})\{1 + \frac{1}{2v_{\lambda'}^2}\} + \frac{exp(-v_{\lambda'}^2)}{\sqrt{\pi} v_{\lambda'}}]}{1 + 2\lambda' \cos\theta + \lambda'^2} d\lambda'$$

where

$$v_{\lambda'} = \gamma [\, 1 - 2\,\beta \frac{\lambda' + \cos\theta}{(\, 1 + 2\,\lambda' \cos\theta + \lambda'^2\,)^{1/2}} + \beta^2\,]^{1/2}$$

$$\gamma = u\sqrt{\alpha}$$

λ' = collision path length normalized by r_O.

Unlike the special case for fast H atoms this integral cannot be solved analytically and inverted. However, we have developed an approximation scheme which yields a single-iteration solution, based on the fact that in realistic cases the numerator within the integral is only a weakly varying function along the path length. The approximation is a two-step predictor corrector type solution. The first step is to make an initial guess whereby we assume that the numerator in the integral is a constant. This accounts for the temperature and relative velocity of the particle near the start of the collision path. With this term as a constant the remaining integral can be done analytically as in Combi and Smyth (1988a). This path length serves as a first guess or predictor of the true path length. As a second step we then replace the numerator of the real integral with its

value at the half-way point along the predicted collision path and proceed to recalculate the a corrected collision path.

This was tested by calculating the collision probability along the path from some point of origin out to infinity both with the new method and by explicit numerical integration. We concentrated on the expected troublesome cases where the method might be expected to do the worst. In the inner part of the coma where the collision paths are all short because the densities are high the method gives almost an exact result. Fortunately in realistic models there are very few particles which have velocity vectors in the regime where the approximation is not as good.

An example of a pathological case would be a radical which is located at 2-5 collision path radii from the nucleus and which has a velocity magnitude equal to the outflow speed but is directed to within an angle of 10 to 30 degrees of the negative radial direction. Note that it is very improbable to generate such radicals as dissociation products of outflowing parents. However, even in this case it is not until the collision probability exceeds 95% that the approximate collision path length begins to diverge only somewhat from an actual collision path integral calculation. The conclusion is thus that only a very small fraction of collisions for only a small fraction of molecules will have some small error in the calculation of collision paths.

Once a collision occurs, we choose a randomized target particle from the background gas, which is a moving Maxwellian. Since it is easier to choose the background gas particle from an isotropic (in angle) moving Maxwellian rather than from the correct relative velocity weighted distribution, we have employed the principle of the 'prejudiced' source - or the skewed probability density distribution of Combi and Smyth (1988a) - where we choose from one distribution and then weight the particle according to the relative magnitude of the real to the assumed probability density distribution. This prevents us from needing to generate look-up tables for complicated multidimensional functions. This also minimizes both the computation times for model runs and development time in changing the model. These new features have been incorporated into the model. These enhancements improve our modeling of the typical cometary radicals and represent an important step toward studying the fundamental kinetic nature of much of the coma.

We are now planning to apply this model to realistic cases of NH_2, C_2 and CN from the analysis portion of the project during the continuation grant of this project.

II.B. Observed Spatial Profile Analysis

Six months into this current project year our goal was the completion of the work and the preparation of a paper which deals with analysis of a number of spatial profiles of [OI] and NH_2 determined from the long-slit CCD spectra of Comet Halley taken by Drs. Uwe Fink, M. DiSanti and A. Schultz at the University of Arizona. A summary of the data appears in Table 1.

Table 1. Summary of Long Slit Spectroscopy of Comet P/Halley

Date 1985-86	r (AU)	Δ (AU)	Number of Spectra
Aug 23	2.84	3.24	3
Aug 24	2.83	3.21	1
Sep 17	2.53	2.49	3
Sep 24	2.43	2.27	3
Oct 20	2.09	1.43	5
Oct 21	2.07	1.40	2
Nov 15	1.72	0.74	9
Dec 8	1.38	0.70	10
Dec 9	1.36	0.72	5
Jan 10	0.87	1.32	13
Jan 11	0.86	1.34	11
Jan 12	0.84	1.36	9
Mar 1	0.72	1.27	15
Mar 2	0.74	1.25	11
Mar 3	0.75	1.22	6
Mar 4	0.76	1.20	6
Mar 5	0.77	1.18	9
Apr 14	1.38	0.43	22
Apr 15	1.39	0.44	19
May 9	1.75	1.05	14
Jun 5	2.13	1.93	6
Jun 6	2.14	1.96	5

r = heliocentric distance in AU

Δ = geocentric distance in AU

Spatial profiles of cometary C_2 and CN were to be produced by Dr. Fink and co-workers for a subsequent paper during the following year (during the next grant period). When we began looking at the spatial profiles from the spectra, it became evident that sky background subtraction procedure adopted by Fink and co-workers was effecting the shape of the spatial profiles far from the nucleus. It is the level at distant locations along the profile which is the most important from the standpoint of inferring lifetimes and scale lengths and constraining model parameters.

Because of these complications Dr. Fink has revised his procedure for performing the sky level assessment and has re-reduced the spatial profiles for all four species from most of the CCD spectra. The result of this has been to push back the publication date of the first paper, which will deal with a simple analysis of the spatial profiles of all four species, until early in the next project year. Whereas, the publication of the second paper, which will deal with a more substantial model analysis concentrating on C_2 and CN will still be finished on the original schedule by the end of the first project year of the follow-up grant.

By the end of this current project year we have received all of the revised spatial profiles for all four species and have performed the first-step Haser model analysis. There are some restrictions regarding the fitted scale lengths and the fitting procedure, which will be discussed here species by species. An Appendix to this report contains all of the observed profiles with best fit Haser models.

II.B.a. [OI]

The forbidden oxygen emission is now believed to originate from oxygen atoms produced in the metastable ^1D state upon photodissociation of their parent molecules. The major sources of $O(^1D)$ atoms are now believed to be H_2O in the inner coma (Biermann and Trefftz 1964) and OH in the outer coma (van Dishoeck and Dalgarno 1984). Roughly 100 seconds after the atoms are produced they emit either the 6300 Å or the 6364 Å photon (in the ratio of 3/1), unless they are produced in the very inner coma (<1000 km) where the ^1D state can be collisionally quenched before a photon emission (Festou and Feldman 1984). The result of this is that the $O(^1D)$ emission is proportional to the H_2O column in the inner coma (<10^5 km) and to the OH column in the outer coma (>10^5 km). Magee-Sauer et al. (1989) have published simple model profiles for the combined source given alternative sets of branching ratios.

The end result is that we expect the spatial distribution of $O(^1D)$ emission to decrease as the inverse of the distance to the nucleus and have a scale length for decay somewhere intermediate between the scale lengths for decay of H_2O and OH. Table 2 gives the results for the $O(^1D)$ profiles. In fact all except one of the spatial profiles is well reproduced by a point source model with a decay scale length, except for the case of December profile where a still very small source

Table 2. Haser Scale Lengths for [OI] Profiles

Date	observed P	observed D	r_H^2 P	r_H^2 D	$r_H^{1.5}$ P	$r_H^{1.5}$ D
Oct	0	49	0	11	0	16
Dec	2.1	330	1.1	175	1.3	205
Jan10	0	40	0	54	0	50
Jan11	0	54	0	77	0	70
Jan11C	0	330	0	446	0	428
Jan12	0	48	0	65	0	62
Mar1	0	-	0	-	0	-
Mar2	0	33	0	60	0	52
May	0	-	0	-	0	-

P = Parent scale length in 10^3 km.

D = Daughter scale length in 10^3 km.

r_H^2 = Reduced to 1 AU by an r_H^2 law

$r_H^{1.5}$ = Reduced to 1 AU by an $r_H^{1.5}$ law

scale length is required for a model fit. This is likely, however, to be a fictitious scale length whereby the flattening is due simply to the irregular activity of the gas production.

Unfortunately, except for the December and the January 11 composite profile (created from a regular exposure and one with a long integration time where the nucleus was masked), it is possible that we are not really seeing the true effective decay scale length but simply the fact that the profile becomes too noisy.before a significant departure from 1/r can be seen. The fact that we do see the 1/r distribution near the nucleus implies that the reduction procedure, the subtraction of of the contribution to the 6300 Å emission from NH_2 and the evaluation of the sky level are all reasonably well done.

II.B.b. NH_2

For NH_2 there just are not many published spatial profiles and determined scale lengths available. It has been suggested in recent, but as yet unpublished results, that the NH_2 spatial distribution is consistent with primary production from the photodissociation of NH_3 (Wyckoff et al. 1990) and with decay primarily through photodissociation producing the visible NH (Schleicher and Millis 1989). Table 3 gives the results for the NH_2 Haser model scale lengths. When reduced to 1 AU by an $r_H^{1.5}$ law. This variation is expected from the combination of photodissociation of a parent molecule, whose lifetime varies as r_H^2, and the approximate $r_H^{-0.5}$ variation in the coma outflow speed from photochemical heating (Combi 1989). Since the NH_2 radicals are produced generally within 10,000 km from the nucleus they are also expect (at least for the heliocentric distances covered) to be thermalized and follow the same outflow speed as the water coma. The straightforward power law fit in r_H in fact agrees with this interpretation.

Given a variation of $r_H^{1.5}$ we find values for the lifetimes of the NH_2 parent and NH_2 , respectively to be 5500 km and 40,000 km. Given an outflow speed, at 1000-10,000 km from the nucleus of about 0.8 km/s for NH_3 this implies a lifetime for NH_3 of 6900 seconds which agrees quite well with the expected value of 7700 seconds (Allen, 1989 private communication). A lifetime for NH_2 with an average velocity closer to 1.0 km/s would yield a lifetime of about 40,000 seconds at 1 AU. Note that for immediate (or nearly immediate) thermalization, the radial motion assumed by the Haser model is quite realistic and and appropriate to first order. OH, on the other hand, is produced much farther from the nucleus and vectorial ejection of the the radicals must be taken into account (Festou 1981). We will test the thermalization of NH_2, in the context of these data, using the new heavy molecule collision algorithm discussed in the previous section of this report.

Table 3. Haser Scale Lengths for NH_2 Profiles

	observed		r_H^2		$r_H^{1.5}$	
Date	P	D	P	D	P	D
Oct	12.2	365	2.8	84	4.1	122
Dec	9.4	109	5.0	58	5.9	68
Jan10	4.0	46.5	5.3	61	4.9	57
Jan11	2.8	59.4	3.4	80	3.5	74
Jan11C	2.6	72.3	3.5	98	3.3	91
Jan12	2.6	63.2	3.7	90	3.4	82
Mar1	4.4	11.9	8.5	23	7.2	19
Mar2	4.6	13.7	8.4	25	7.2	22
May	21.4	52.9	7.0	17	9.2	23

P = Parent scale length in 10^3 km.

D = Daughter scale length in 10^3 km.

r_H^2 = Reduced to 1 AU by an r_H^2 law

$r_H^{1.5}$ = Reduced to 1 AU by an $r_H^{1.5}$ law

II.B.c. CN

The last summary of pre-Halley spatial profiles for CN was done by Combi and Delsemme (1986). In that paper we found that from data for a number of comets that the parent Haser scale length was about 2 x 10^4 km and seemed to vary as $r_H^{1.5}$ which is (like NH_2 above) consistent with production from the photodissociation of a parent molecule. The daughter scale length seemed to be of order 3.2 x 10^5 km at 1 AU but the heliocentric distance dependence was always too irregular to determine. For the new spatial profiles from comet Halley we find that some of the profiles do not extend to large enough distances from the nucleus to enable the determination of both scale lengths. For these we assume a value consistent with the value at 1 AU which scales with a square law dependence. Since the daughter scale length is very long compared with the parent value, the parent scale length determined this way is only weakly dependent on the assumed daughter value anyway. For some we can and have determined both scale lengths. Table 4 gives the list of best fit Haser models for the CN profiles.

The values determined so far are reasonably consistent with our pre-Halley summary, although we are now in the process of assembling the results from a number of investigations in which CN scale lengths were determined for Halley. These results will be compiled with our new data results in the second paper to be finished by the end of the first year of the continuation project to this one (Combi, Fink and Di Santi 1991, in preparation).

II.B.d. C_2

Perhaps the most surprising results come from the Haser model analysis of the C_2 profiles. In the pre-Halley summary (Combi and Delsemme 1986), we found that both the parent 1.6 x 10^4 km) and daughter (1.1 x 10^5 km) scale lengths varied as the square of the heliocentric distance. In this new data we have profiles which extend both very close to the nucleus and fairly far away, as compared generally with the data we had in our 1986 summary. In the old data the profiles never did go as close to the nucleus.

For all of the new C_2 profiles, we require a Haser model where the parent and daughter scale lengths are equal. Furthermore, the value varies as the square of the heliocentric distance as opposed to the slower variation implied by the CN, and NH_2. Note that for the old summary Combi and Delsemme (1986) found a ratio of about 7 between the daughter and the parent. The reason an equal scale length model is required is because all of the profiles are very flat near the nucleus and turn over very rapidly. This behavior has been noted by other investigators (Cochran 1985; Wyckoff et al. 1988) going as far back as Delsemme and Miller (1971).

Various suggestions for the unusual appearance of the C_2 profiles including a 2-step photodissociation (grandparent-to-parent-C_2) and a grain source have been made (see Wyckoff et

Table 4. Haser Scale Lengths for CN Profiles

	observed		r_H^2		$r_H^{1.5}$	
Date	P	D	P	D	P	D
Oct	-	-	-	-	-	-
Dec	24	550	12.4	293	14.9	343
Jan10	22	413	29	546	27.1	509
Jan11	25	376	34	508	31	471
Jan11C	31	(400)	23	(540)	39	(501)
Jan12	21	(375)	14.8	(531)	27	(487)
Mar1	15	730	29	1408	25	1195
Mar2	45	45	82	82	71	71
May	44	(980)	14	(320)	19	138

P = Parent scale length in 10^3 km.

D = Daughter scale length in 10^3 km.

r_H^2 = Reduced to 1 AU by an r_H^2 law

$r_H^{1.5}$ = Reduced to 1 AU by an $r_H^{1.5}$ law

Values in parentheses are daughter scale lengths assumed either from the value on an adjacent day or from the 3.2×10^5 km extrapolated to the actual heliocentric distance.

al. 1988). Continued work on the unusual appearance and behavior of the C_2 profiles and their heliocentric distance dependence will be one of the principal subjects of the second paper to be written later this year (Combi. Fink and Di Santi, 1991, in preparation). Table 5 shows the list of the best fit Haser scale lengths.

Table 5. Haser Scale Lengths for C_2 Profiles

Date	Observed	r_H^2
Oct	255	59
Dec	107	57
Jan10	40	53
Jan11	41	55
Jan11C	44	59
Jan12	39	55
Mar1	26	50
Mar2	28	51
May	284	93

r_H^2 = Reduced to 1 AU by an r_H^2 law

For all C_2 profiles the parent and daughter scale lengths are equal and in units of 10^3 km.

III. References

Biermann, L. and Trefftz, E. Uber die Mechanismen der Ionisation und der Anregung in Kometen Atmospheren. *Zs. f. Astrophys.* **59**, 1-28, 1964

Cochran, A.L. Nonequilibrium Chemical Analysis of the Coma of Comet P/Stephan-Oterma. *Icarus* **62**, 82-96, 1985.

Combi, M.R. Neutral Cometary Atmospheres. III. The Acceleration of Cometary CN by Solar Radiation Pressure. *Astrophys. J.*, **241**, 831, 1980.

Combi, M.R. .Sources of Cometary Radicals and Their Jets: Gases or Grains. *Icarus* **71**, 178, 1987.

Combi, M.R. The Outflow Speed of the Coma of Halley's Comet. *Icarus* **81**, 41, 1989.

Combi, M.R. and A.H. Delsemme. Neutral Cometary Atmospheres. V. C_2 and CN in Comets. *Astrophys. J.*, **308**, 472, 1986

Combi, M.R. and W.H. Smyth. Monte Carlo Particle Trajectory Models for Neutral Cometary Gases. I. Models and Equations. *Astrophys. J.* **327**, 1026, 1988.

Combi, M.R. and W.H. Smyth. Monte Carlo Particle Trajectory Models for Neutral Cometary Gases. II. The Spatial Morphology of the Lyman-alpha Coma. *Astrophys. J.* **327**, 1044, 1988.

Delsemme, A.H. and D.C Miller. Physico-Chemical Phenomena in Comets-IV. The C_2 Emission of Comet Burnham (1960II). *Planet. Space Sci.* **19**, 1259-1274, 1971.

Festou, M.C. The Density Distribution of Natural Compounds in Cometary Atmospheres. I. Models and Equations. *Astron. Astrophys.* **95**, 69-79, 1981.

Festou, M., and P.D. Feldman.. Forbidden oxygen lines in comets. *Astron. Astrophys.* **103**, 154-159, 1981.

Fink, Uwe, and M.A. DiSanti. The Production Rate and Spatial Distribution of H_2O for comet P/Halley. *Astrophys. J.* (submitted), 1990.

Fink, Uwe, M. DiSanti, A. Schultz and M. Combi. Emission Profiles for Comet P/Halley. *Bull. A.A.S.* **20**, 828 (abstract), 1988.

Magee-Sauer, K., F.L. Roesler, F. Scherb, and J. Harlander. Spatial Distribution of $O(^1D)$ from Comet Halley. *Icarus* **76**, 88-99, 1988.

Schleicher, D.G. and R.L. Millis. Revised scale lengths for cometary NH. *Astrophys. J.* **94**, 1008-1016, 1989.

Tegler, S. and S. Wyckoff. NH_2 Fluorescence Efficiencies and the NH_3 Abundance in Comet Halley. *Astrophys. J.* **343**, 395-405, 1989.

van Dishoeck, E.F. and A. Dalgarno. The dissociation of OH and OD in comets by solar radiation. *Icarus* **59**, 305-313, 1984.

Wyckoff, S., S. Tegler, and P.A. Wehinger.. Abundances in comet Halley at the time of the spacecraft encounters. *Astrophys. J.* **325**, 927-938, 1988

Wyckoff, S., S.C. Tegler, L. Engel, M. Womack, A. Ferro, and B. Peterson. Ammonia and N Abundances in Comets. Bull. Amer. Astr. Soc. **22**, 1088 (abstract), 1990.

APPENDIX

A Comparison of Haser Models vs. Observed Profiles

The following is a set of Figures for all of the determined spatial profiles of $O(^1D)$, NH_2, CN and C_2. Each figure is a plot of Log Brightness (Arbitrary Units) vs. Log Distance from the Nucleus in (km). For some of the figures the fitted scale lengths are printed at the bottom. Below is a Table containing the coded name for each of the spatial profiles giving the date and species. The coded name contains the name of species also. In some cases the spatial profile was created from the sums of spectra taken on consecutive days (e.g. Oct 20-21, Dec 8-9). There is a set of profiles taken on January 11 (denoted as Jan 11C) which was created as a composite of a "normal" spectrum plus a "masked" spectrum of long integration time which yields a better signal-to-noise ratio than the normal spectra alone. The orbital geometry parameters are given in Table 1 in the main body of this report.

Table A.1. Identification of Spatial Profile Name Codes

Date 1985-1986	$O(^1D)$	$NH_2(0,8,0)$	$C_2(1\text{-}0)$	CN(1-0) (red)
Oct 20-21	i85oicsu	i85n08sb	i85c2sum	i85cn1su.
Dec 8-9	k190oicd	k85n08su	k190c2cd	k190cncd
Jan 10	a174oib	a174nh8	a174c2	a174cn1
Jan 11	janoiasu	jann08su	janc2sum	jancn1su
Jan11C	j11oiasu	j11n08cd	j11c2cbd	j11cn1cd
Jan 12	j12oiasu	j12n08su	j12c2sum	j12cn1su
Mar 1	m01oibsu	m01nh8su	m01c2sum	m01cn1su
Mar 2	m02oibsu	m02nh8su	m02c2sum	m02cn1su
May 9	e86oisum	e86n08su	e86c2sum	e86cn1su

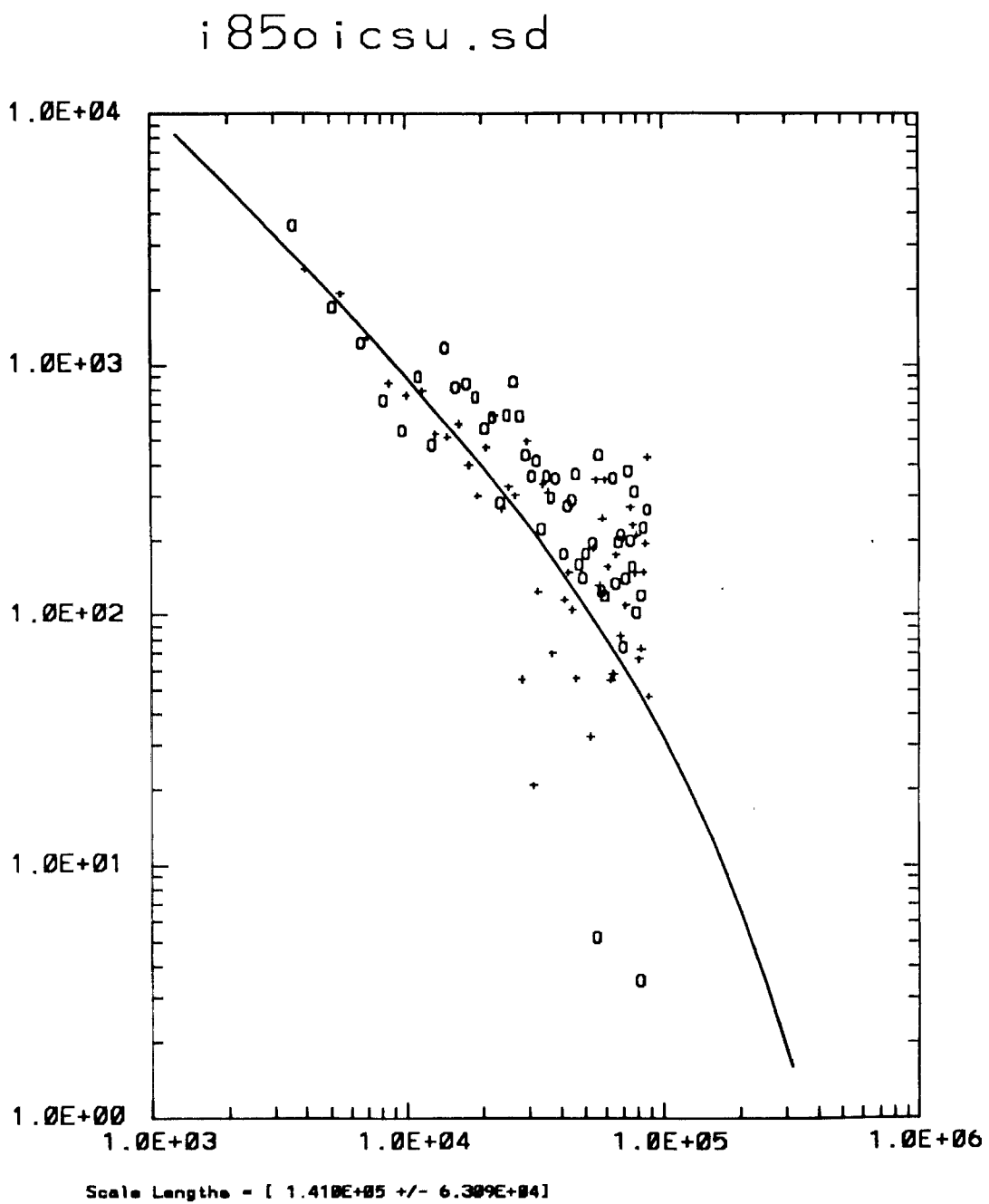
i85oicsu.sd
1.0E+04
1.0E+03
1.0E+02
1.0E+01
1.0E+00
1.0E+03
1.0E+04
1.0E+05
1.0E+06
Scale Lengths = [1.410E+05 +/- 6.309E+04]

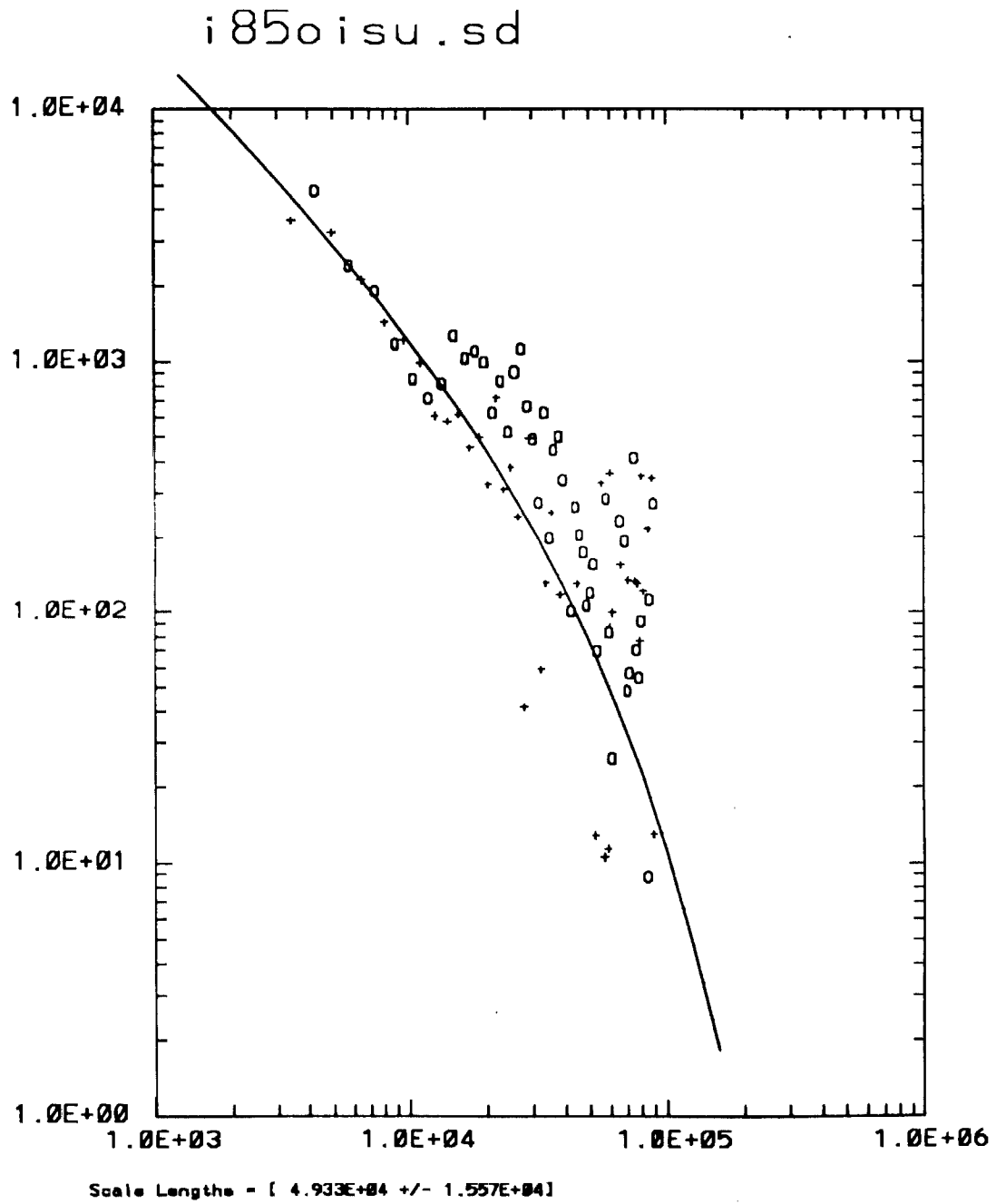
i85oisu.sd
1.0E+04
1.0E+03
1.0E+02
1.0E+01
1.0E+00
1.0E+03
1.0E+04
1.0E+05
1.0E+06
Scale Lengths = [4.933E+04 +/- 1.557E+04]

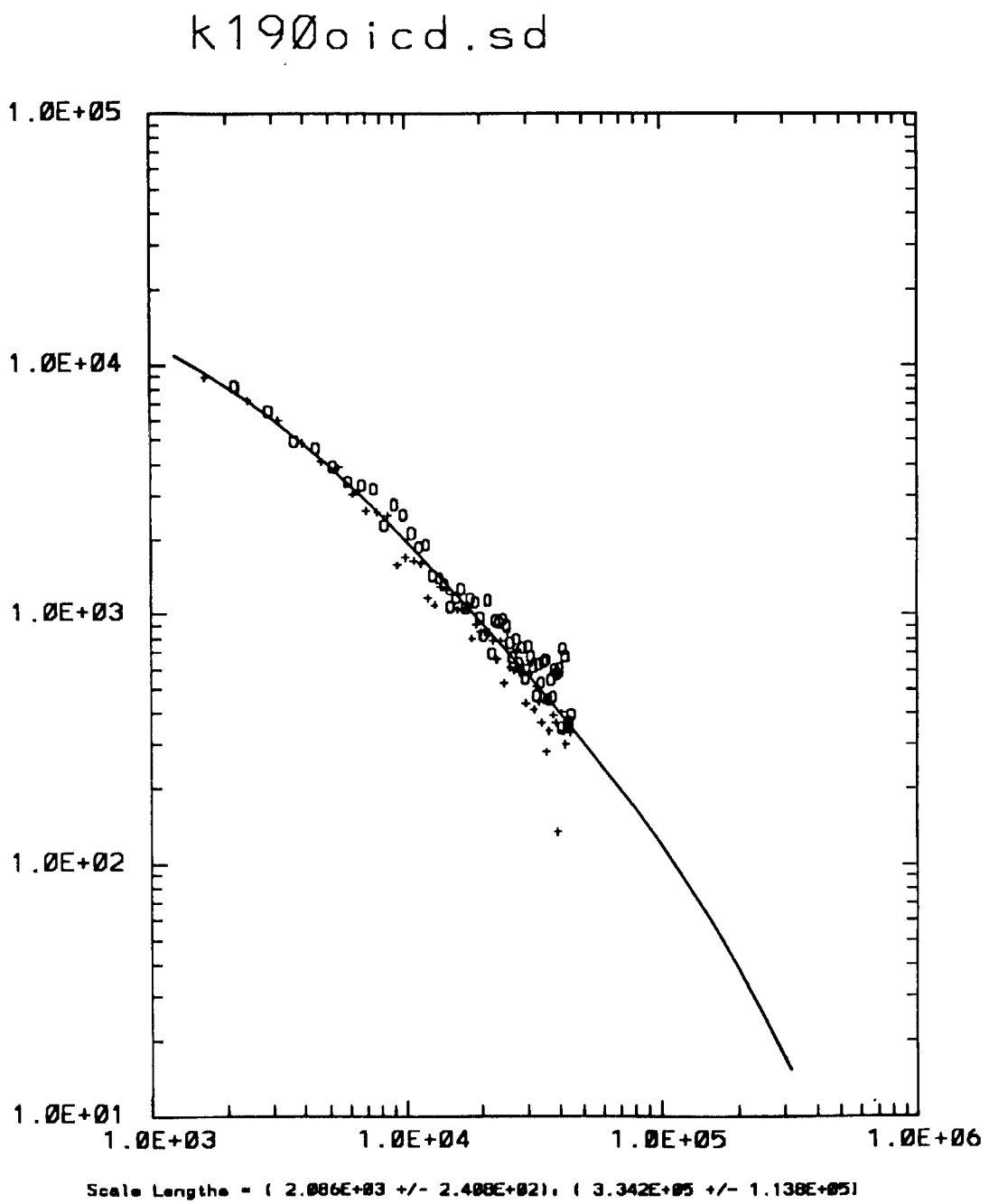
k190oicd.sd
1.0E+05
1.0E+04
1.0E+03
1.0E+02
1.0E+01
1.0E+03
1.0E+04
1.0E+05
1.0E+06
Scale Lengths = (2.086E+03 +/- 2.408E+02), (3.342E+05 +/- 1.138E+05)

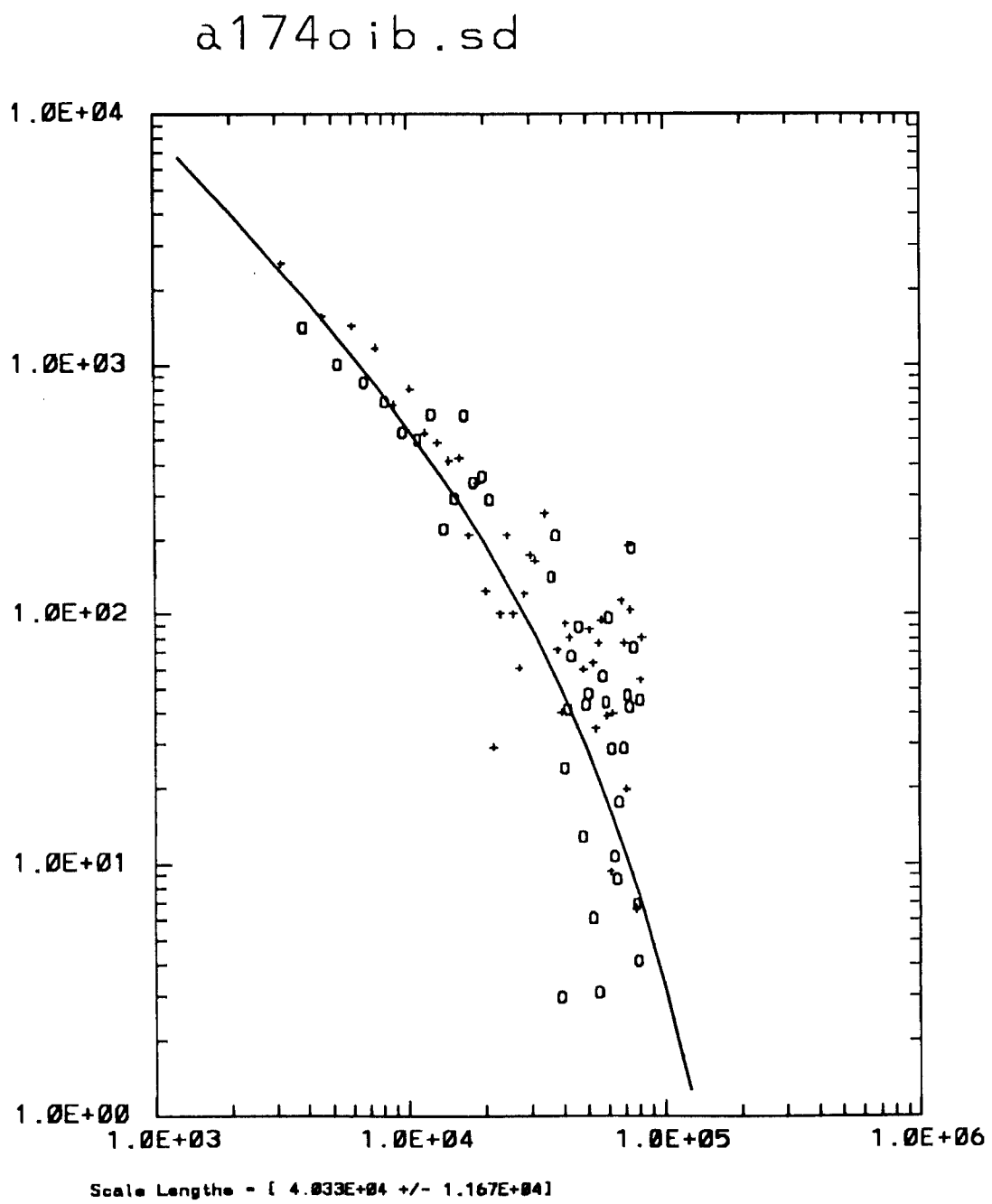
a174oib.sd
1.0E+04
1.0E+03
1.0E+02
1.0E+01
1.0E+00
1.0E+03
1.0E+04
1.0E+05
1.0E+06
Scale Lengths = [4.033E+04 +/- 1.167E+04]

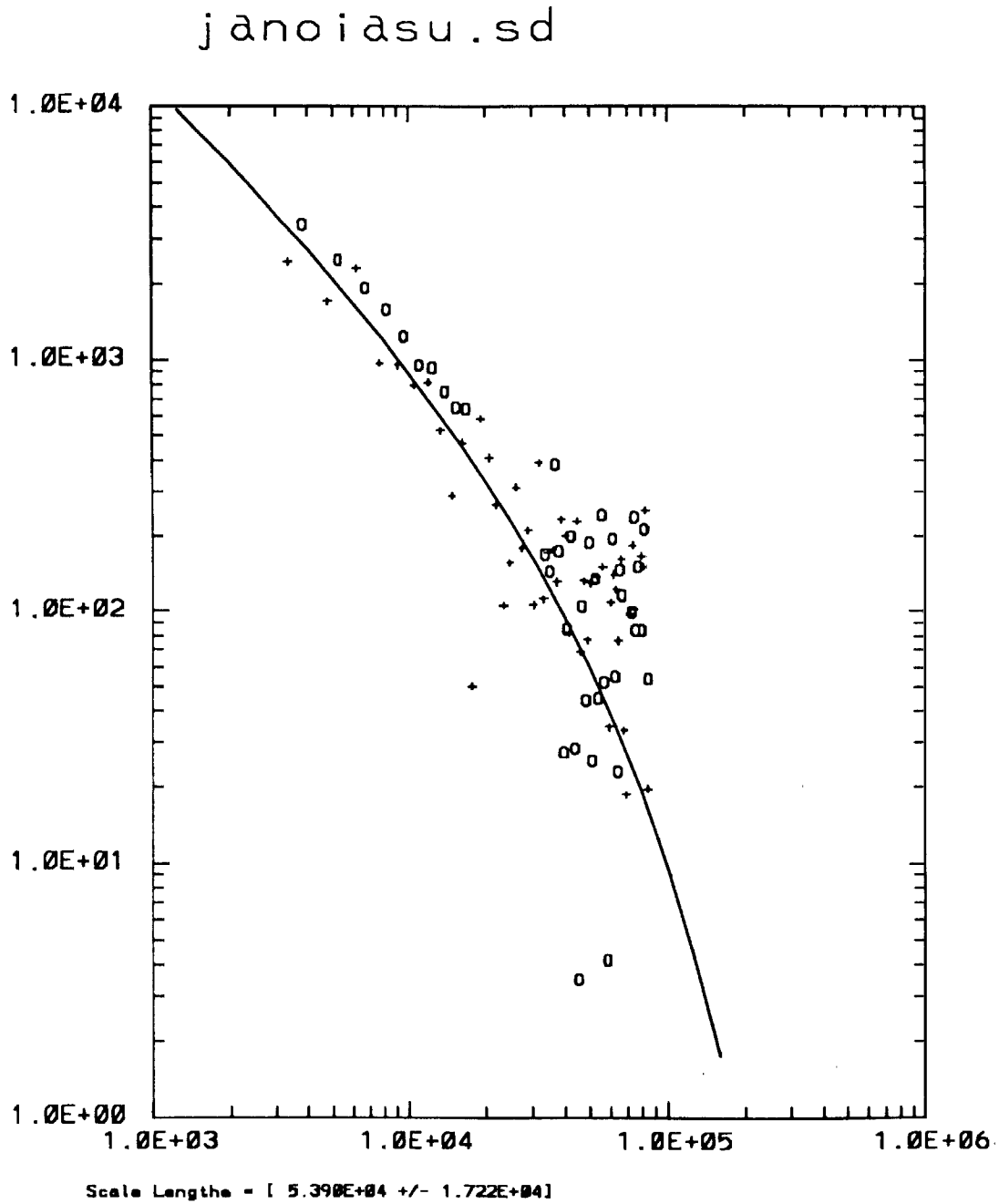
janoiasu.sd
1.0E+04
1.0E+03
1.0E+02
1.0E+01
1.0E+00
1.0E+03
1.0E+04
1.0E+05
1.0E+06
Scale Lengths = [5.390E+04 +/- 1.722E+04]

j11oiacd.sd

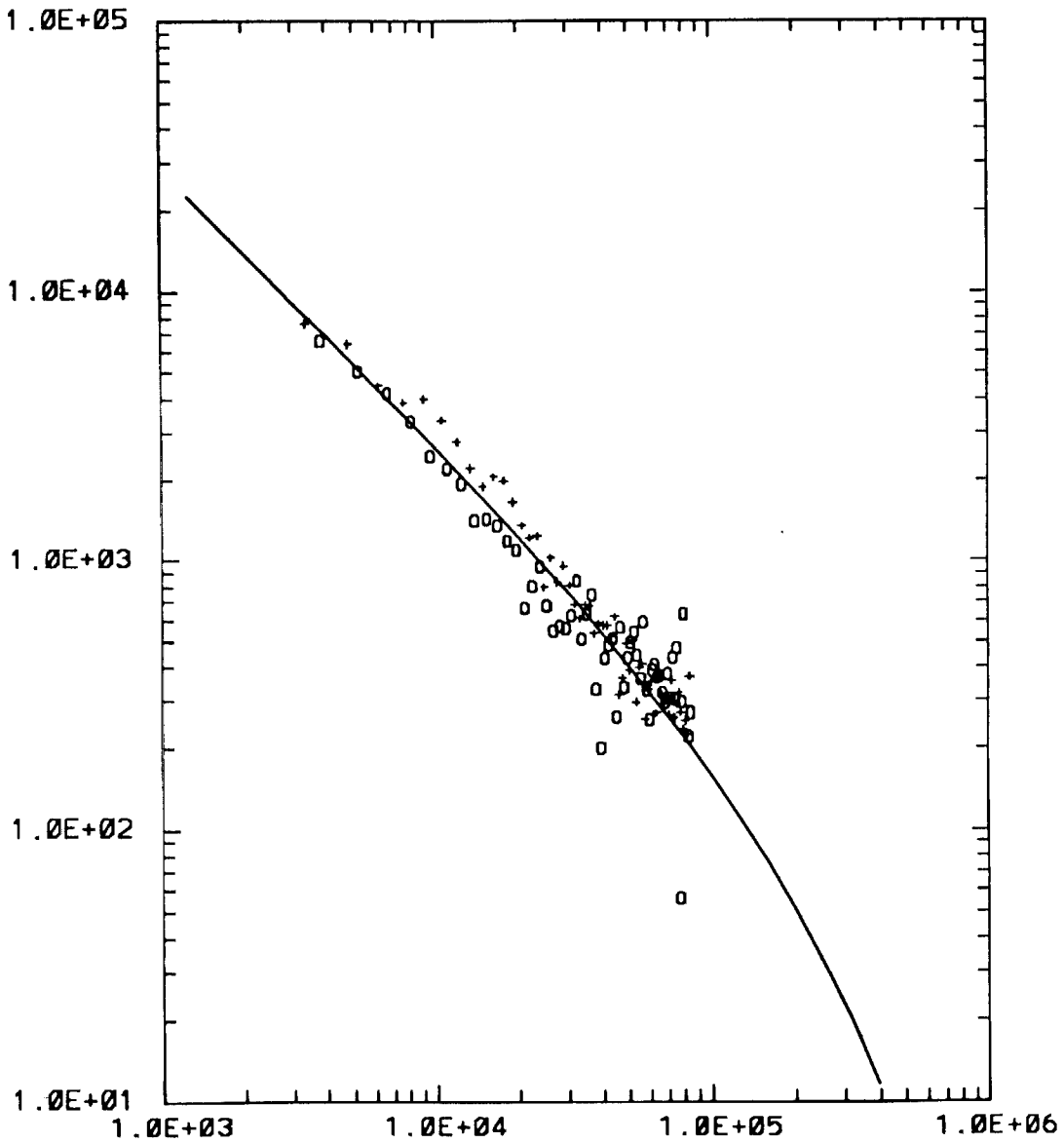

Scale Lengths = [3.300E+05 +/- 9.911E+04]

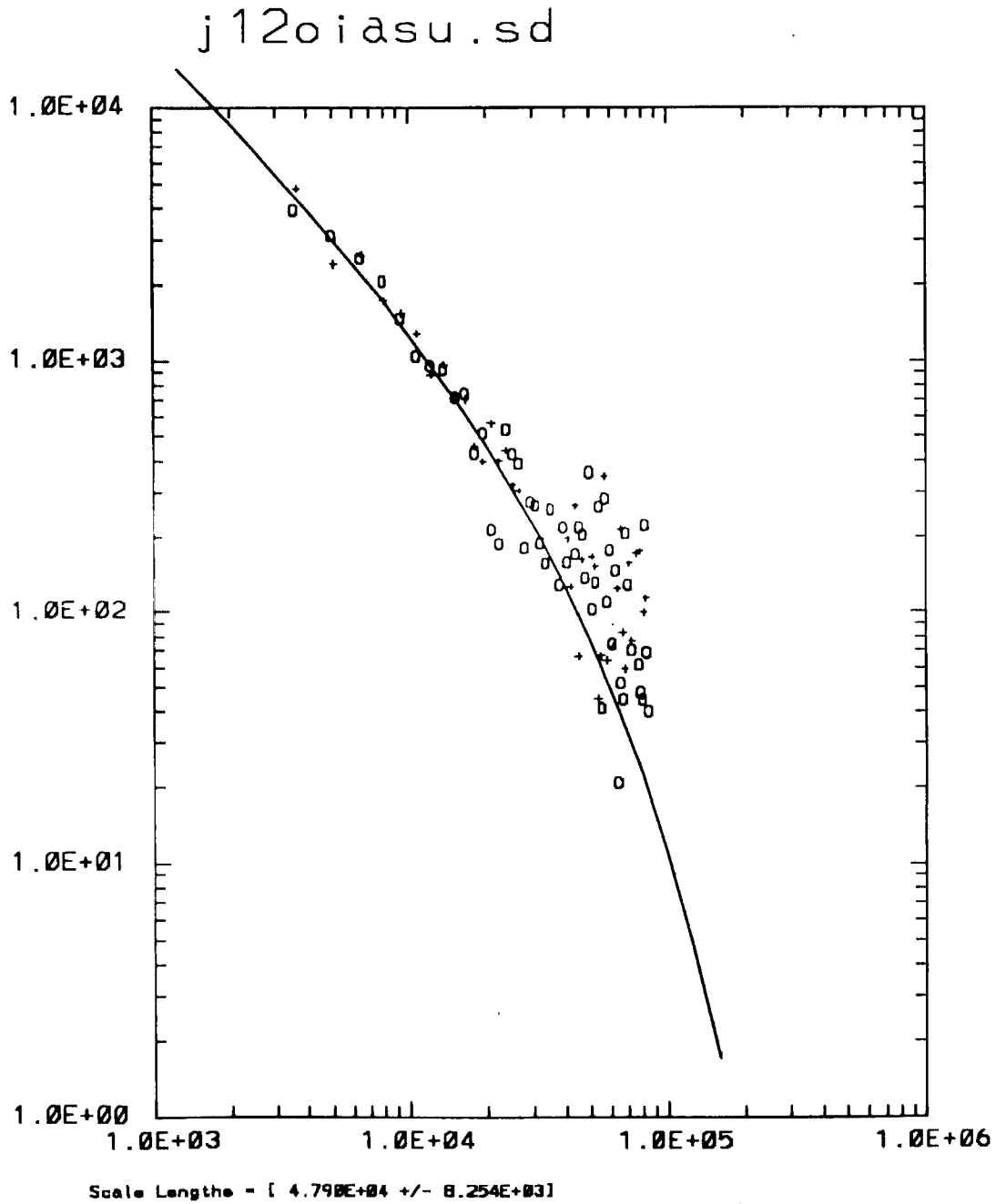
j12oiasu.sd
1.0E+04
1.0E+03
1.0E+02
1.0E+01
1.0E+00
1.0E+03
1.0E+04
1.0E+05
1.0E+06
Scale Lengths = [4.790E+04 +/- 8.254E+03]

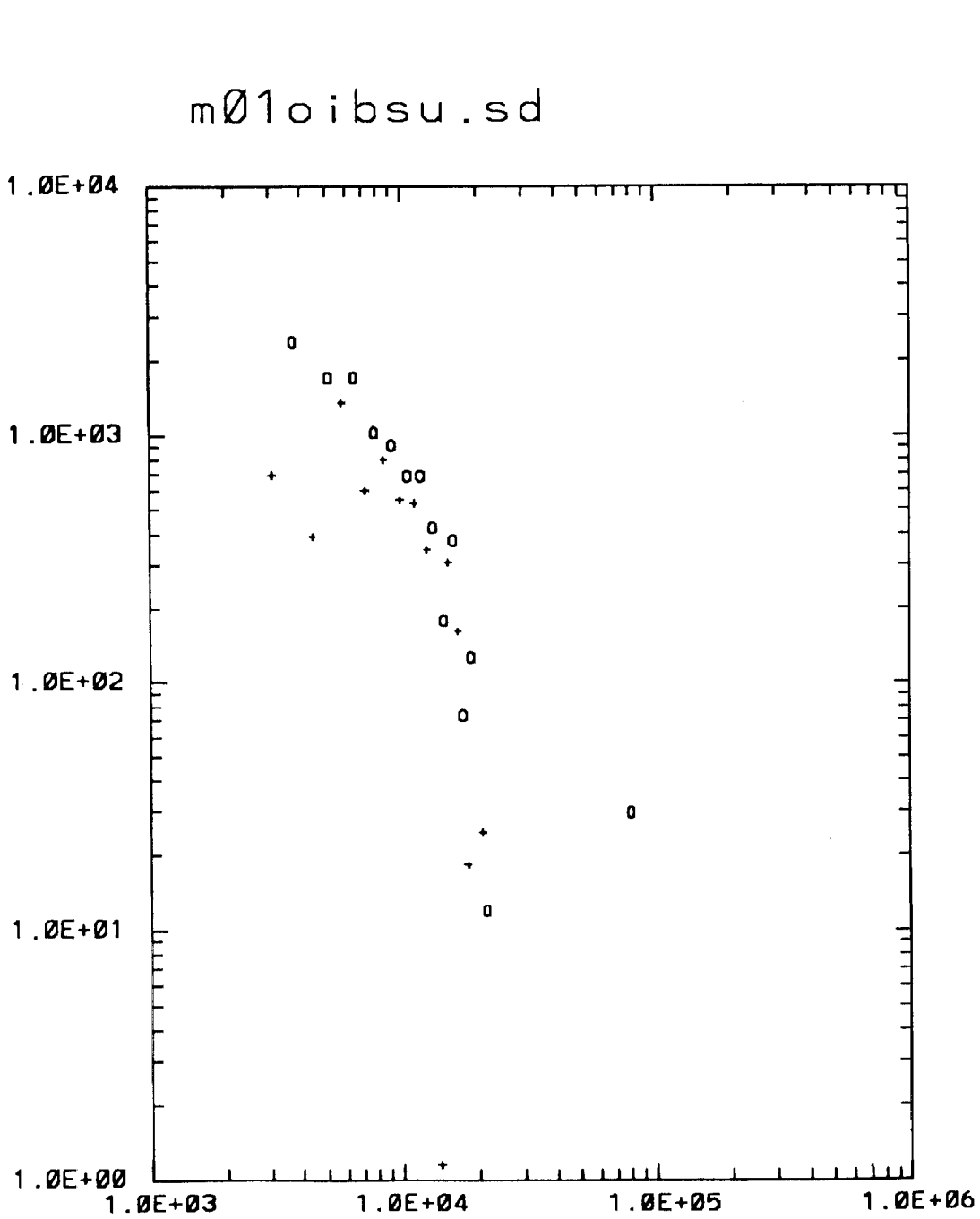
m01oibsu.sd
1.0E+04
1.0E+03
1.0E+02
1.0E+01
1.0E+00
1.0E+03
1.0E+04
1.0E+05
1.0E+06

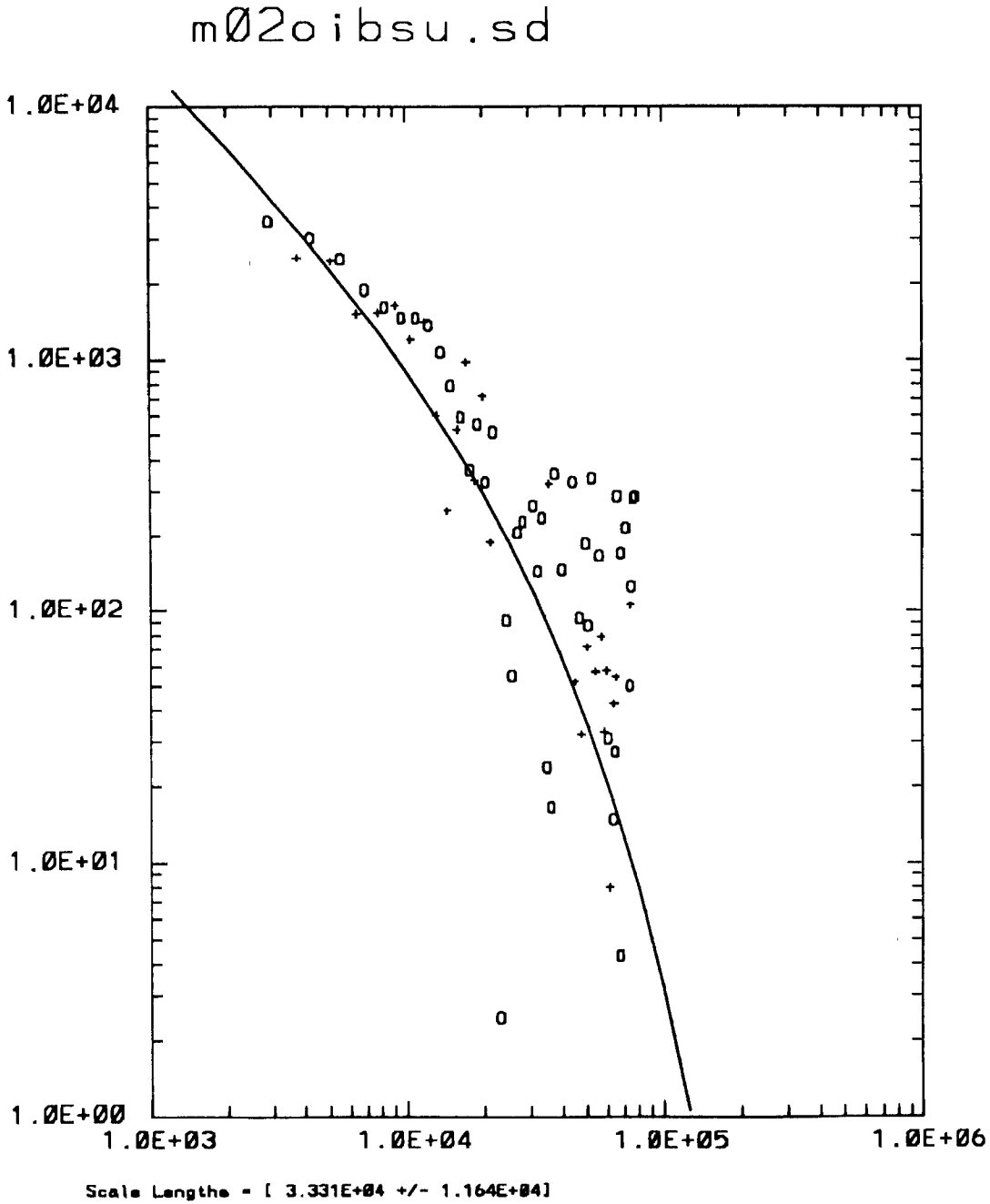
m02oibsu.sd
1.0E+04
1.0E+03
1.0E+02
1.0E+01
1.0E+00
1.0E+03
1.0E+04
1.0E+05
1.0E+06
Scale Lengths = [3.331E+04 +/- 1.164E+04]

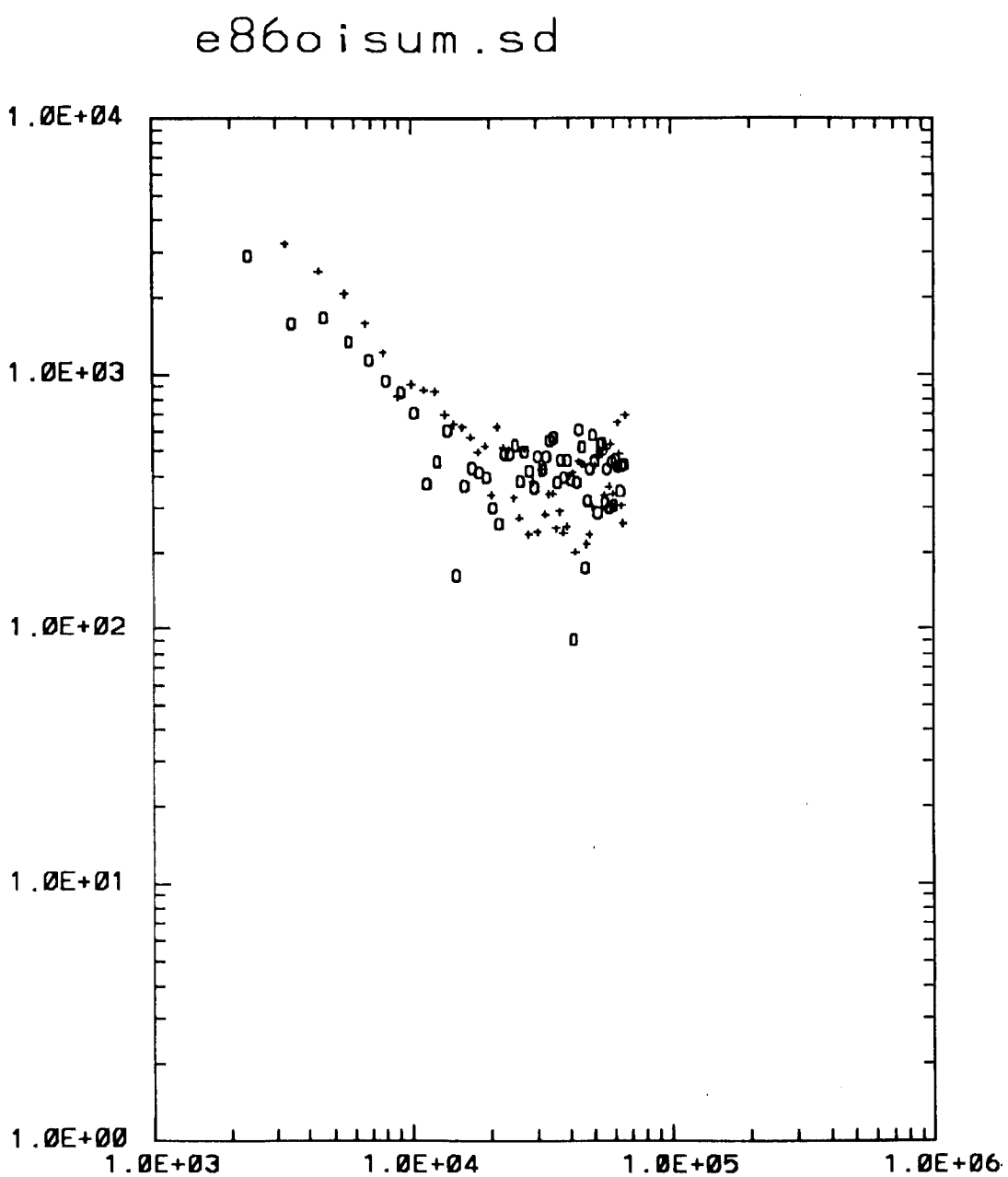
e86oisum.sd
1.0E+04
1.0E+03
1.0E+02
1.0E+01
1.0E+00
1.0E+03
1.0E+04
1.0E+05
1.0E+06

i85n08sb.sd

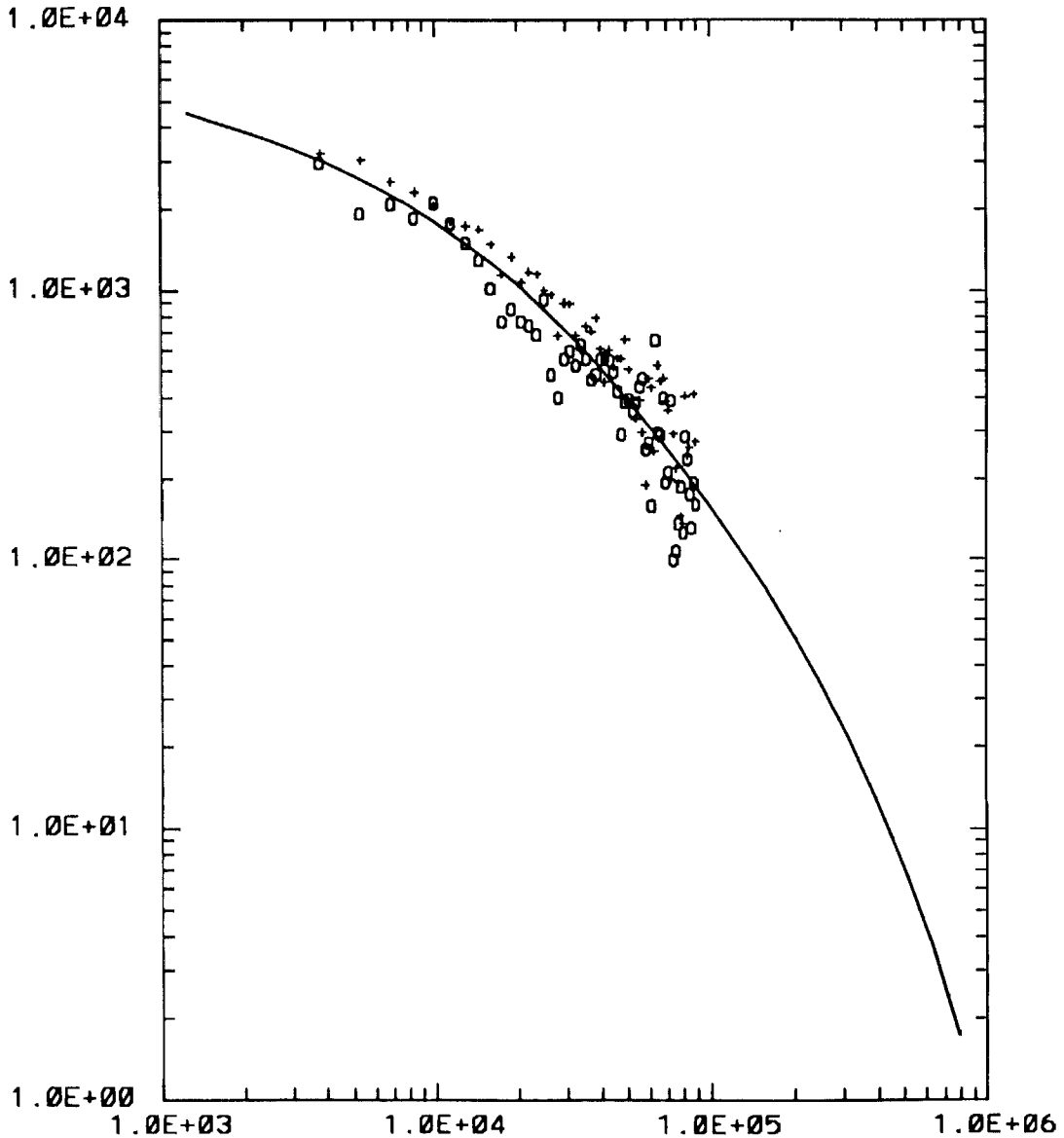

Scale Lengths = (1.220E+04 +/- 3.077E+03); (3.649E+05 +/- 2.581E+05)

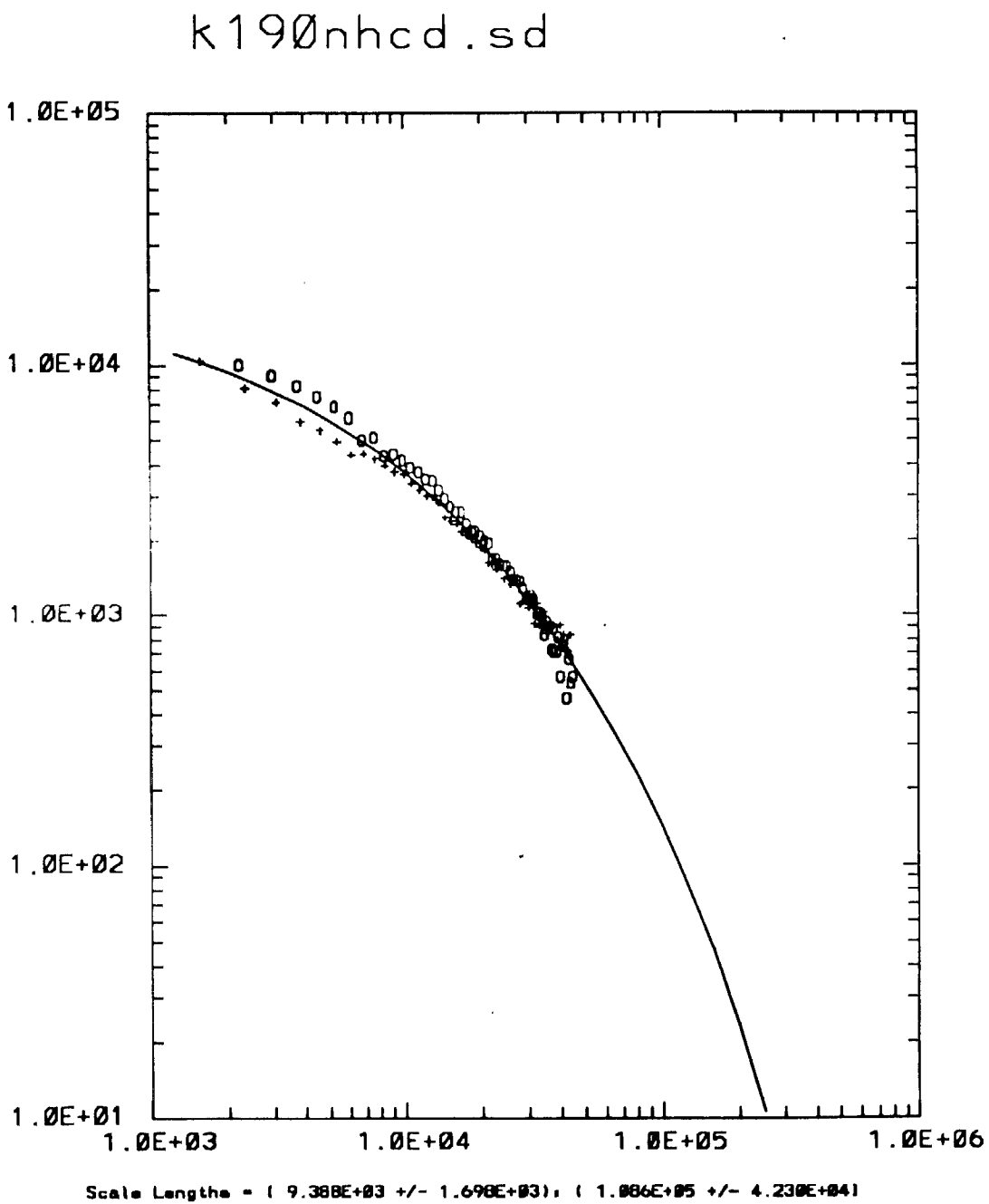
k190nhcd.sd
1.0E+05
1.0E+04
1.0E+03
1.0E+02
1.0E+01
1.0E+03
1.0E+04
1.0E+05
1.0E+06
Scale Lengths = (9.388E+03 +/- 1.698E+03): (1.886E+05 +/- 4.230E+04)

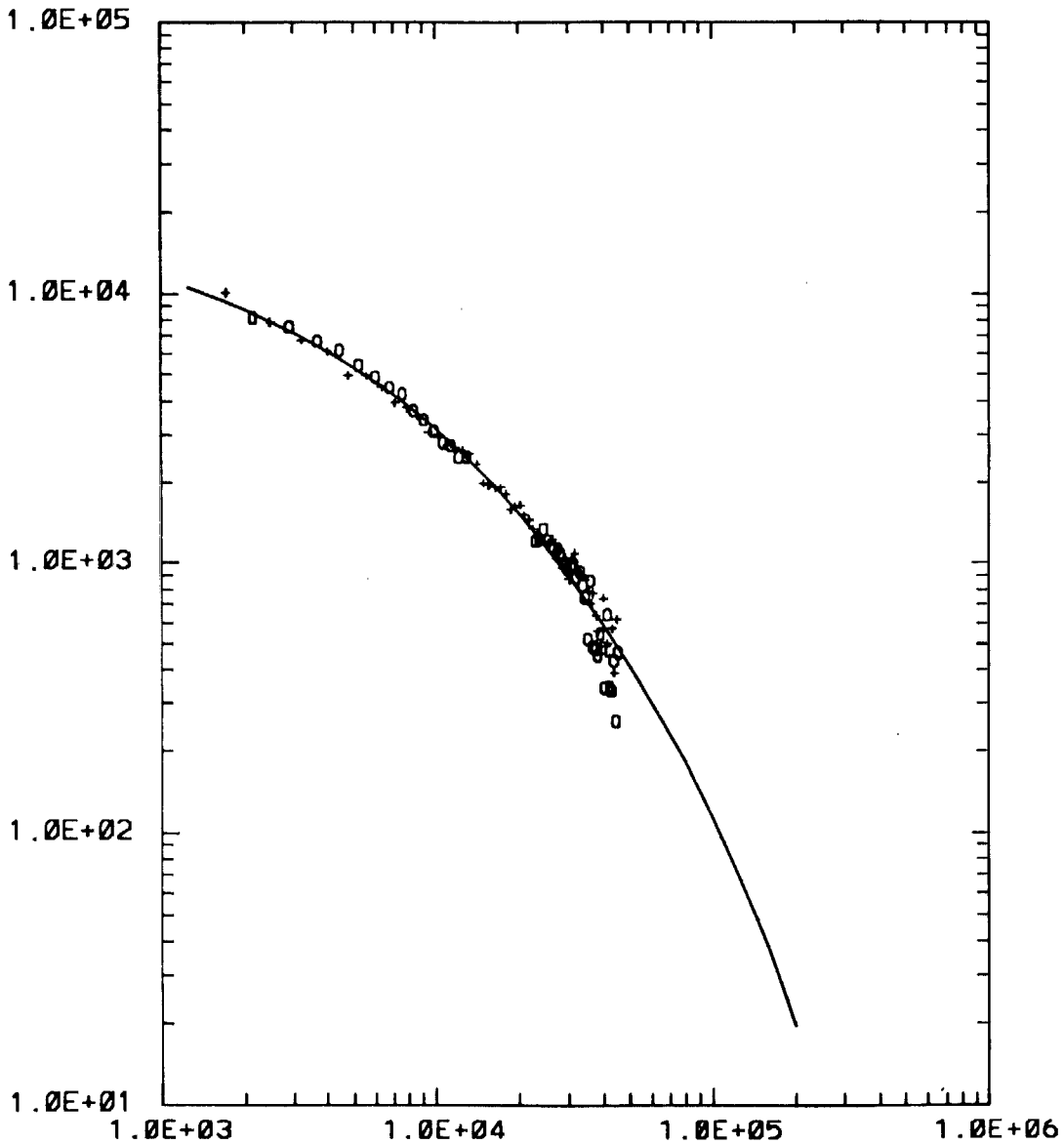
k85n08su.sd
1.0E+05
1.0E+04
1.0E+03
1.0E+02
1.0E+01
1.0E+03
1.0E+04
1.0E+05
1.0E+06
Scale Lengths = (6.969E+03 +/- 6.280E+02), (1.150E+05 +/- 2.139E+04)

a174nh8.sd

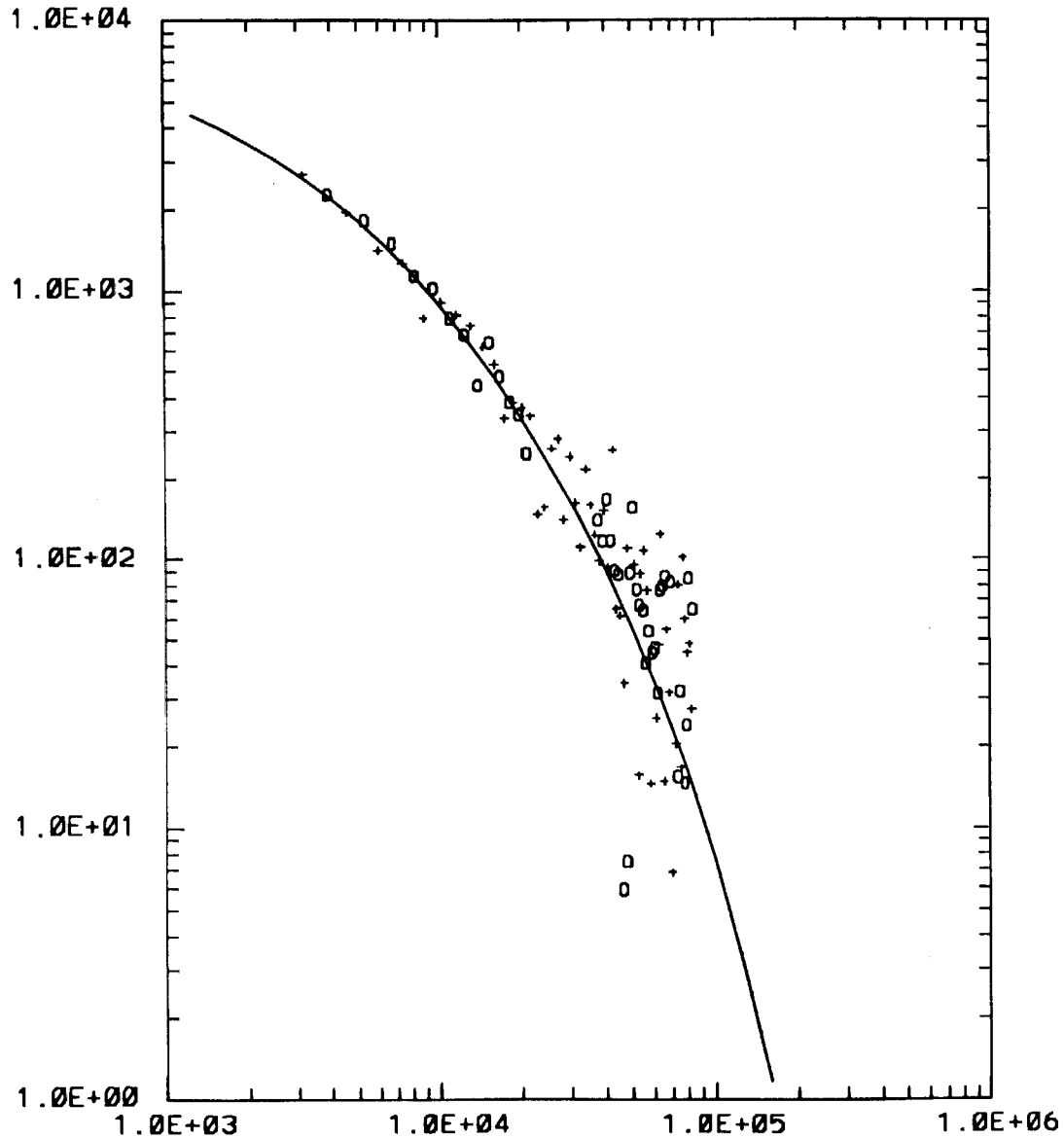

Scale Lengths = (3.979E+03 +/- 8.731E+02), (4.650E+04 +/- 7.807E+03)

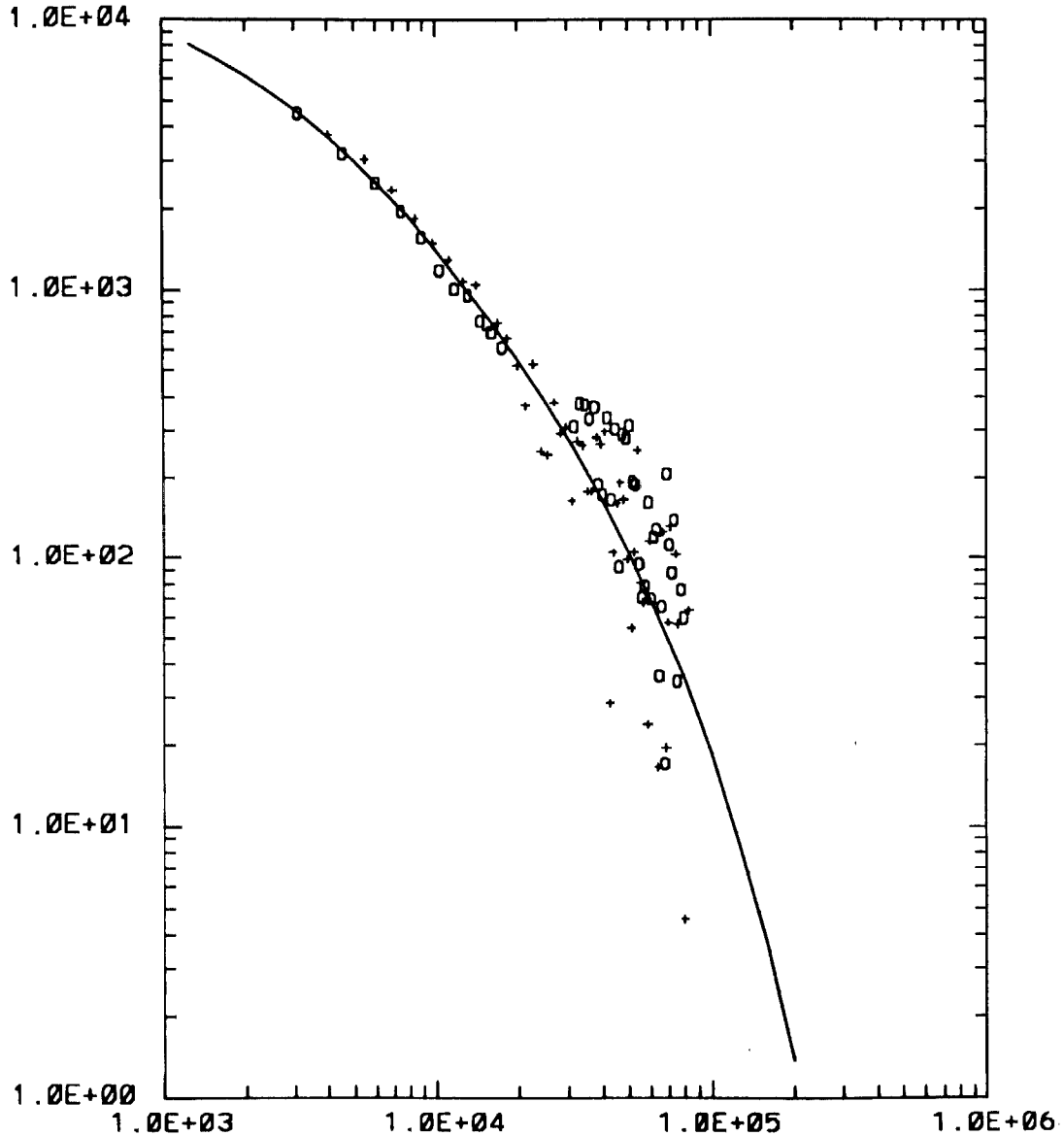
jann08su.sd
1.0E+04
1.0E+03
1.0E+02
1.0E+01
1.0E+00
1.0E+03
1.0E+04
1.0E+05
1.0E+06
Scale Lengths = (2.777E+03 +/- 6.511E+02): (5.944E+04 +/- 8.856E+03)

j11n08cd.sd

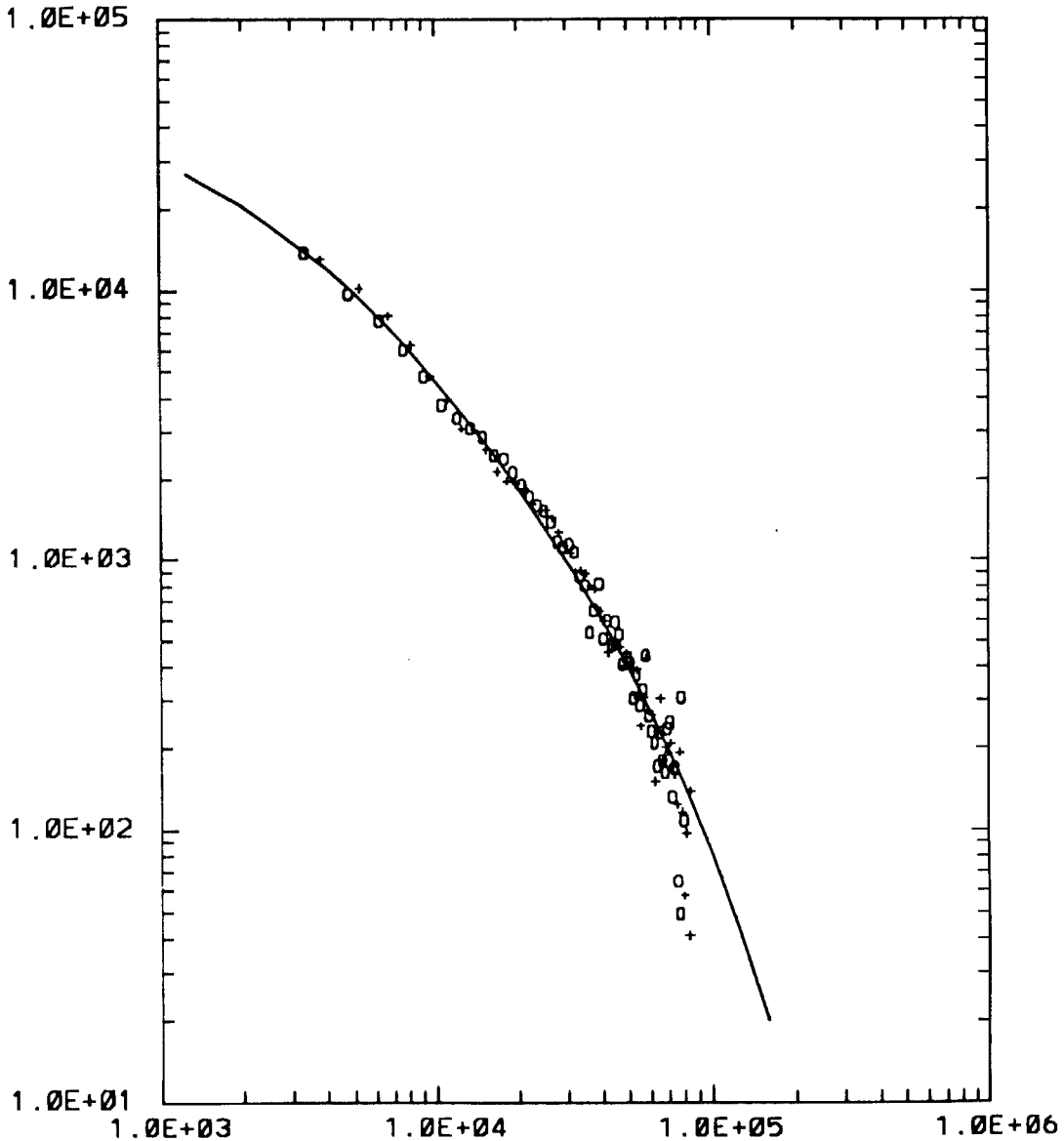

Scale Lengths = (2.558E+03 +/- 4.032E+02), (7.231E+04 +/- 6.833E+03)

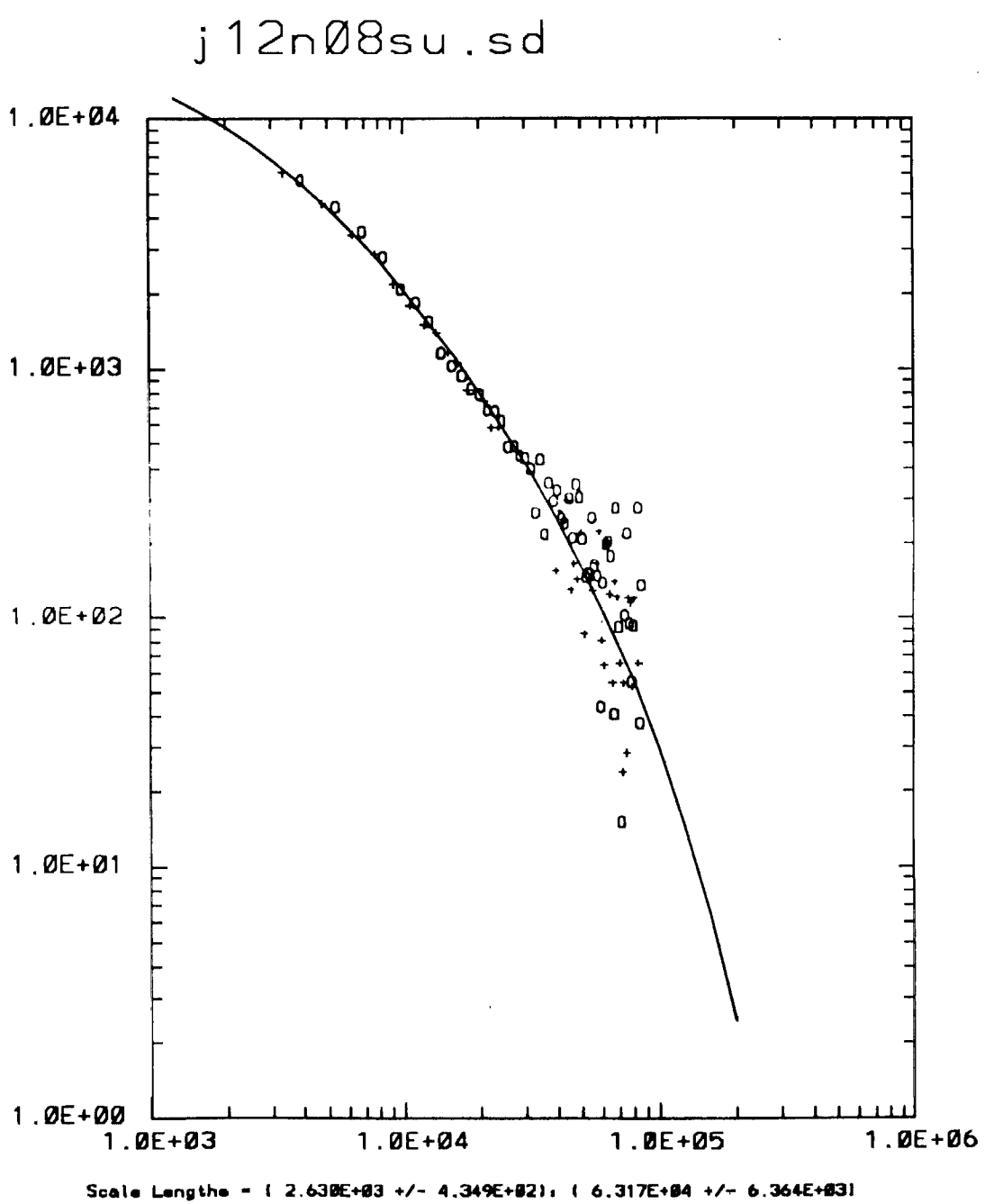
j12nØ8su.sd
1.ØE+04
1.ØE+03
1.ØE+02
1.ØE+01
1.ØE+00
1.ØE+03
1.ØE+04
1.ØE+05
1.ØE+06
Scale Lengths = (2.630E+03 +/- 4.349E+02): (6.317E+04 +/- 6.364E+03)

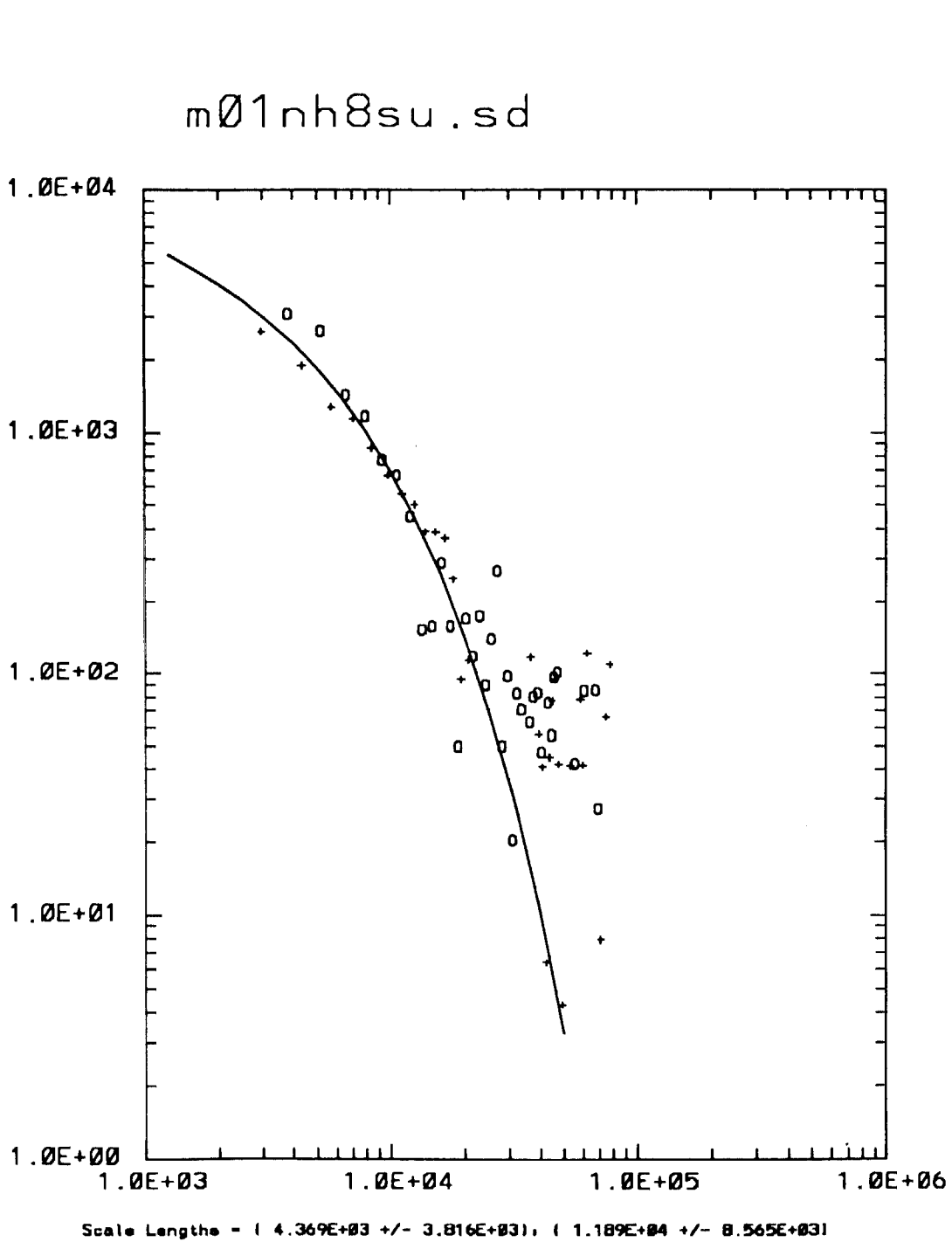
m01nh8su.sd
1.0E+04
1.0E+03
1.0E+02
1.0E+01
1.0E+00
1.0E+03
1.0E+04
1.0E+05
1.0E+06
Scale Lengths = (4.369E+03 +/- 3.816E+03), (1.189E+04 +/- 8.565E+03)

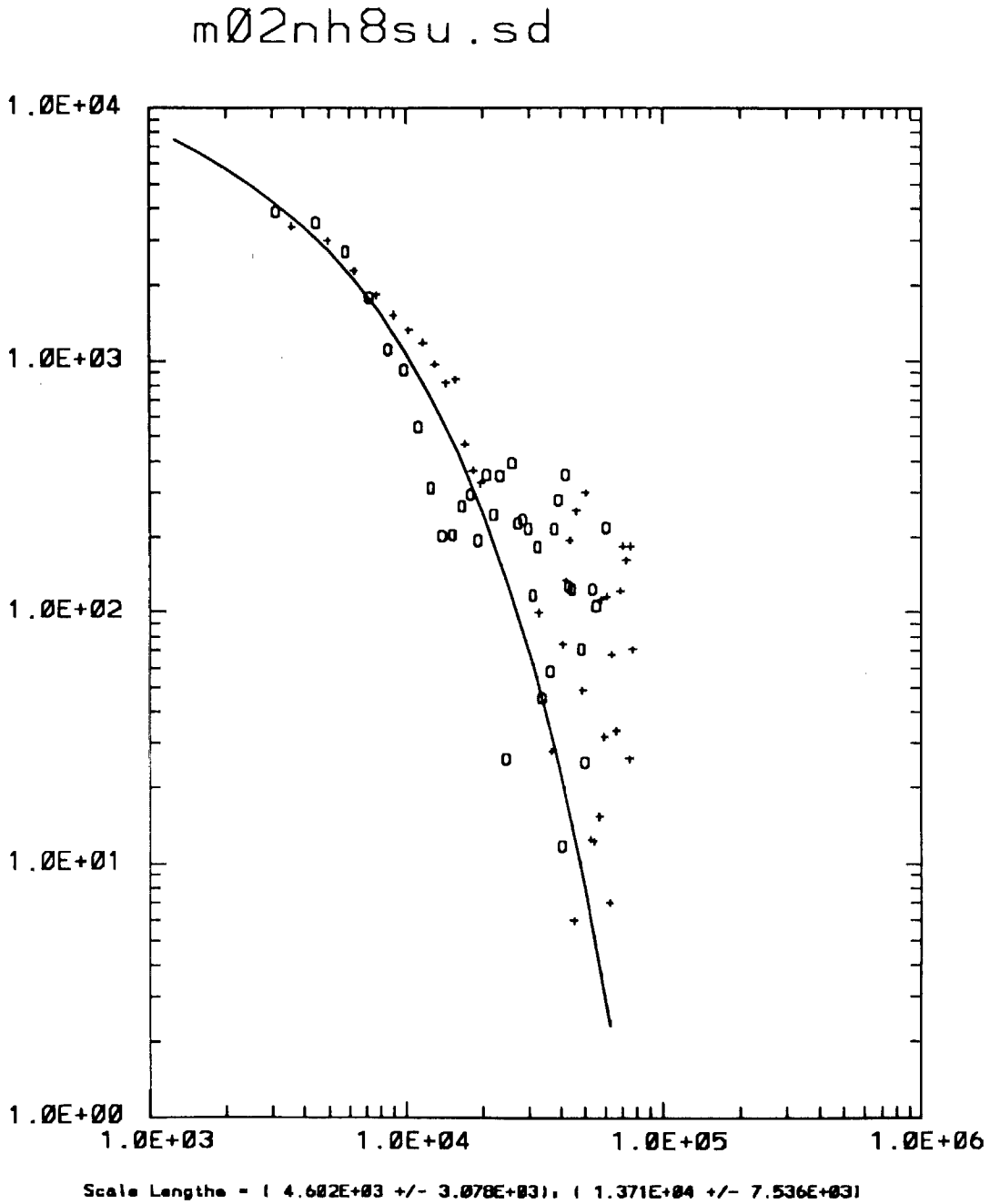
m02nh8su.sd
1.0E+04
1.0E+03
1.0E+02
1.0E+01
1.0E+00
1.0E+03
1.0E+04
1.0E+05
1.0E+06
Scale Lengths = (4.602E+03 +/- 3.078E+03), (1.371E+04 +/- 7.536E+03)

e86n08su.sd

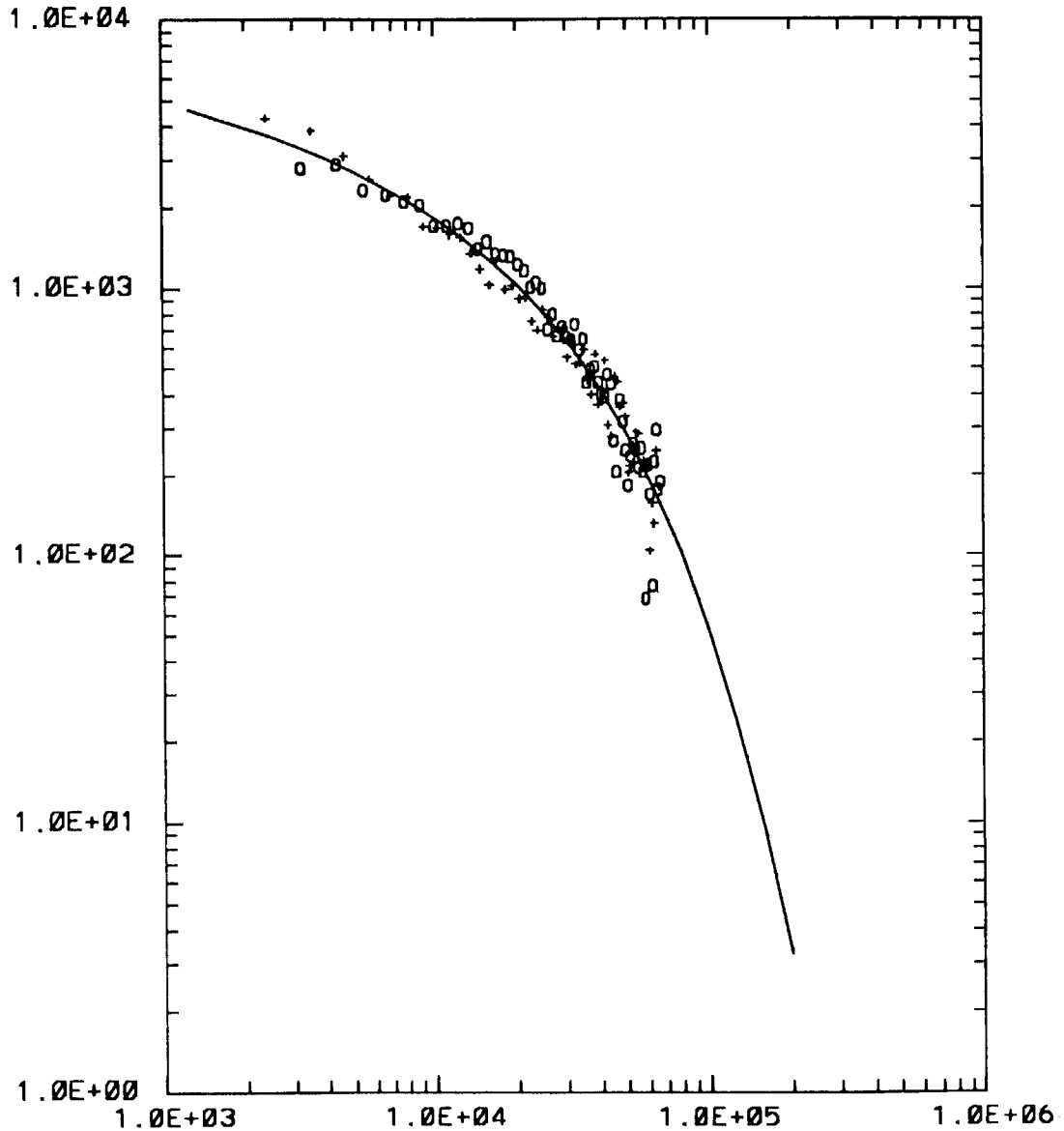

Scale Lengths = (2.139E+04 +/- 9.555E+03); (5.293E+04 +/- 2.903E+04)

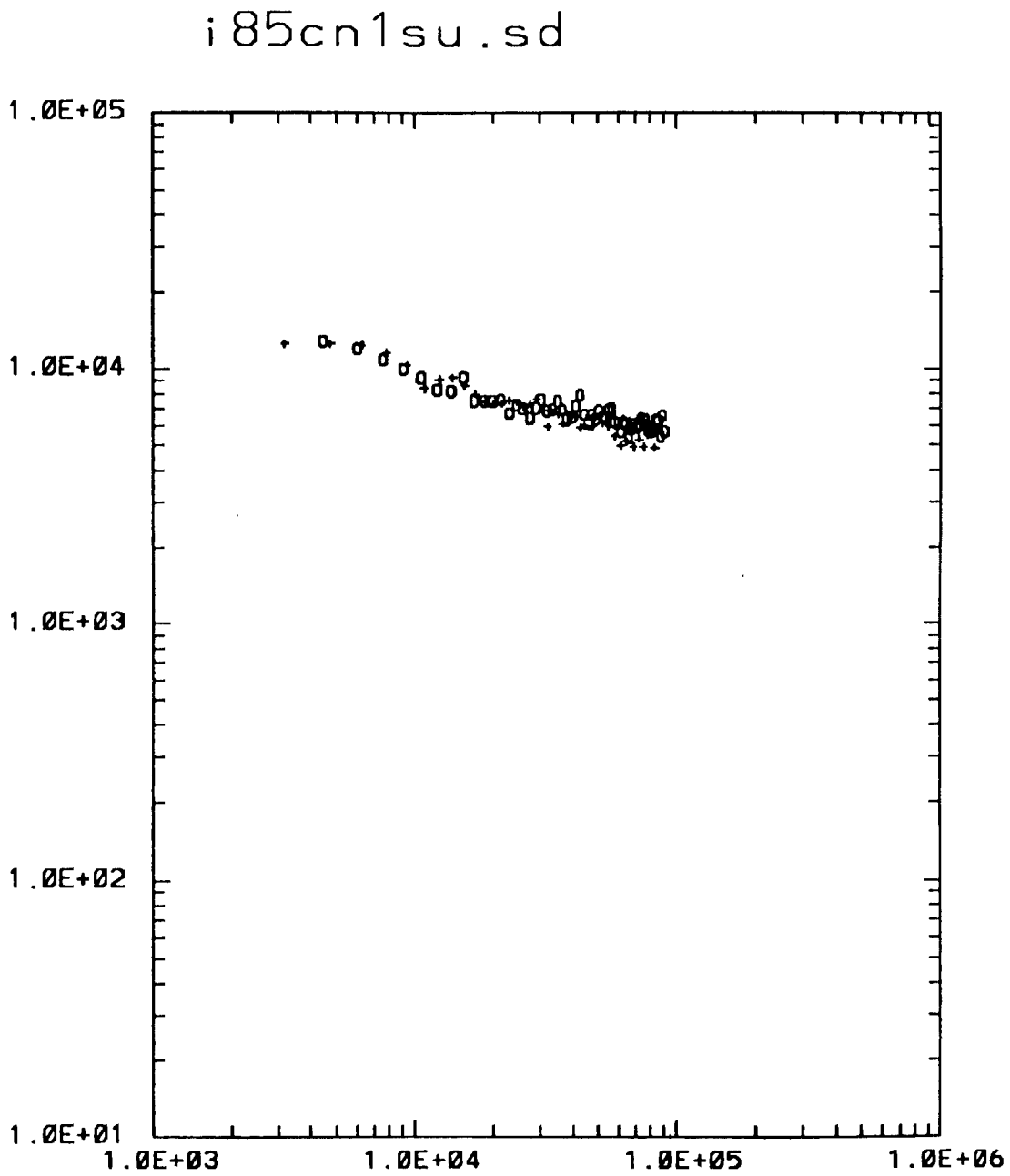
i85cn1su.sd
1.0E+05
1.0E+04
1.0E+03
1.0E+02
1.0E+01
1.0E+03
1.0E+04
1.0E+05
1.0E+06

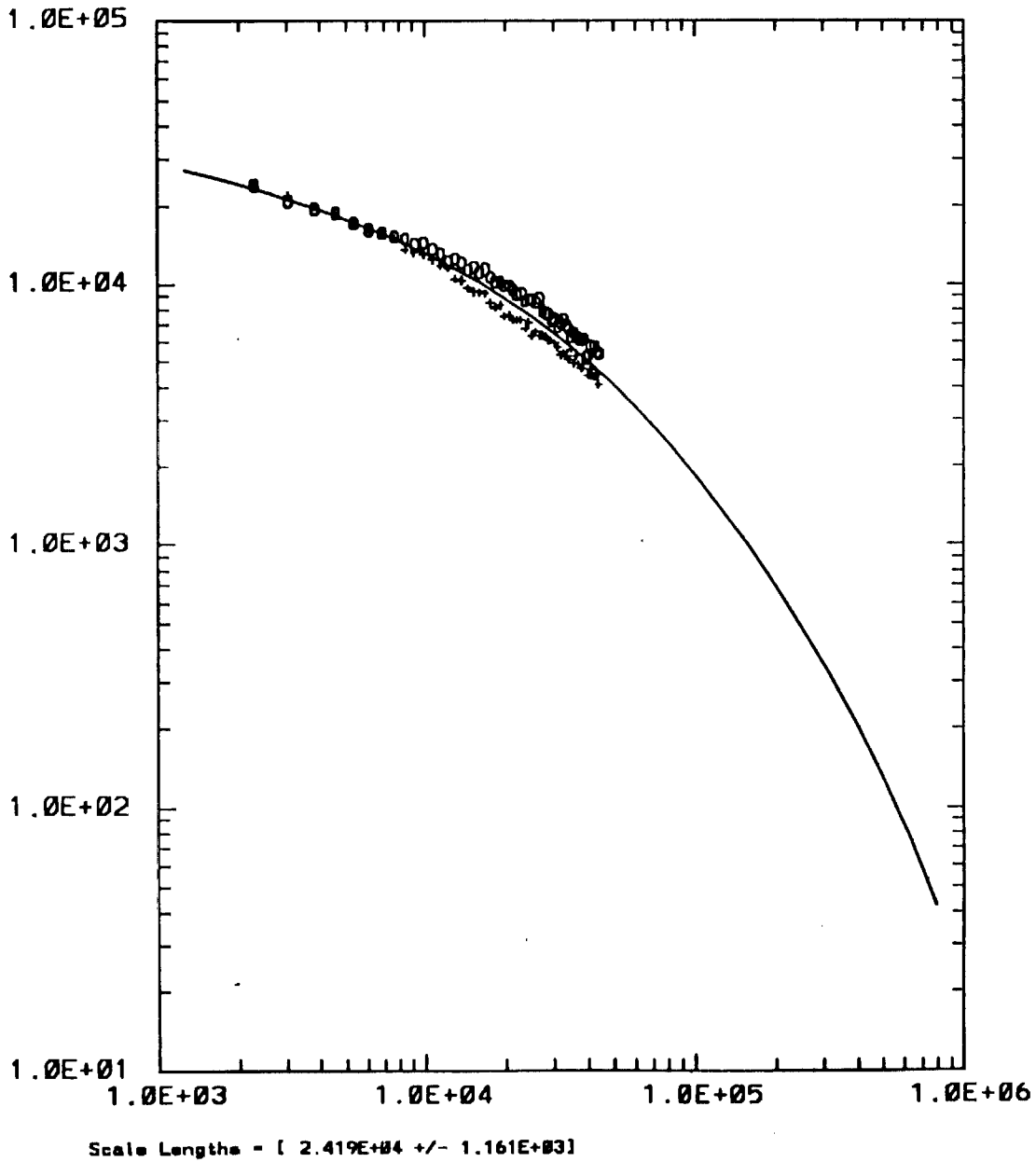
k190cncd.sd
1.0E+05
1.0E+04
1.0E+03
1.0E+02
1.0E+01
1.0E+03
1.0E+04
1.0E+05
1.0E+06
Scale Lengths = [2.419E+04 +/- 1.161E+03]

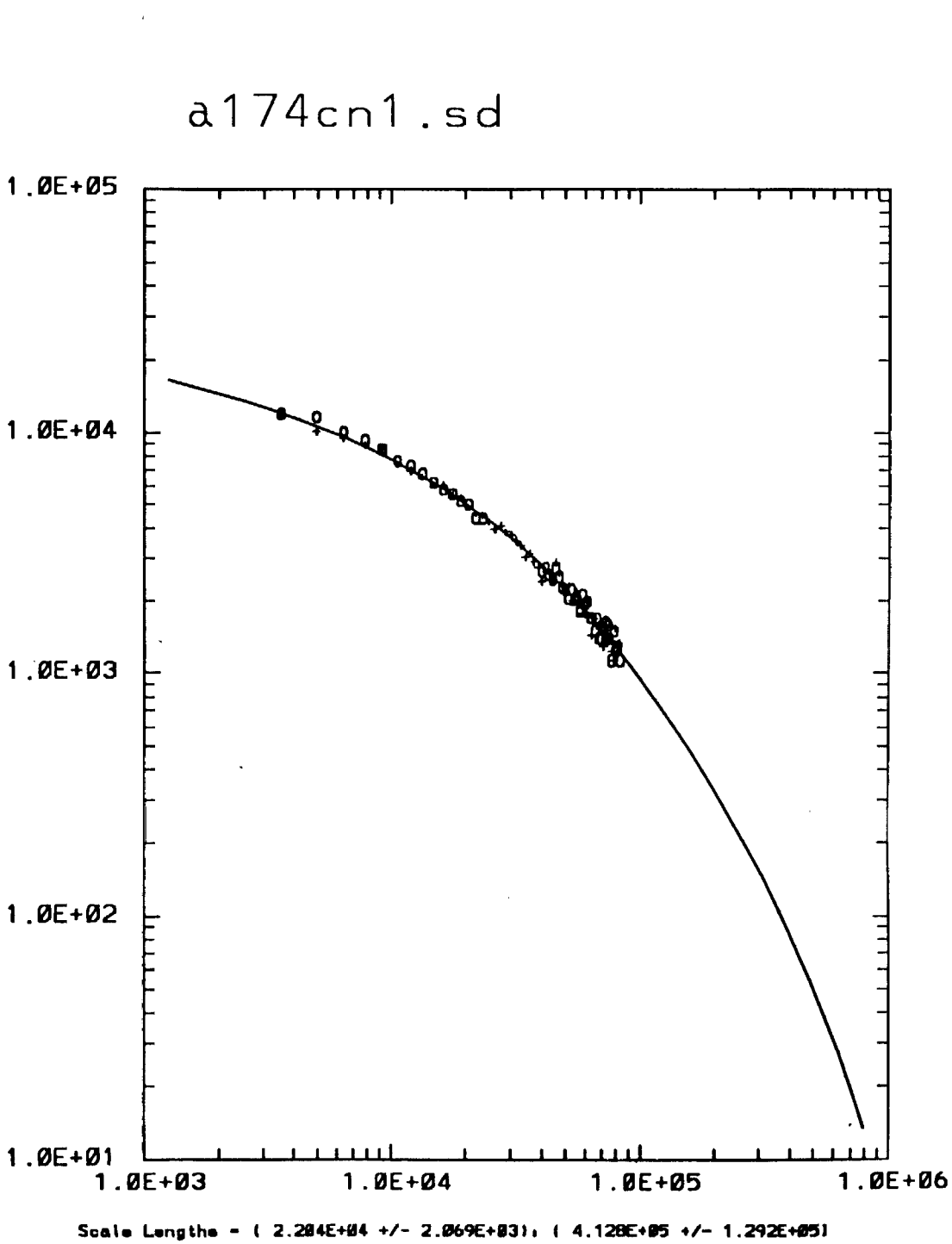
a174cn1.sd
1.0E+05
1.0E+04
1.0E+03
1.0E+02
1.0E+01
1.0E+03
1.0E+04
1.0E+05
1.0E+06
Scale Lengths = (2.284E+04 +/- 2.069E+03), (4.128E+05 +/- 1.292E+05)

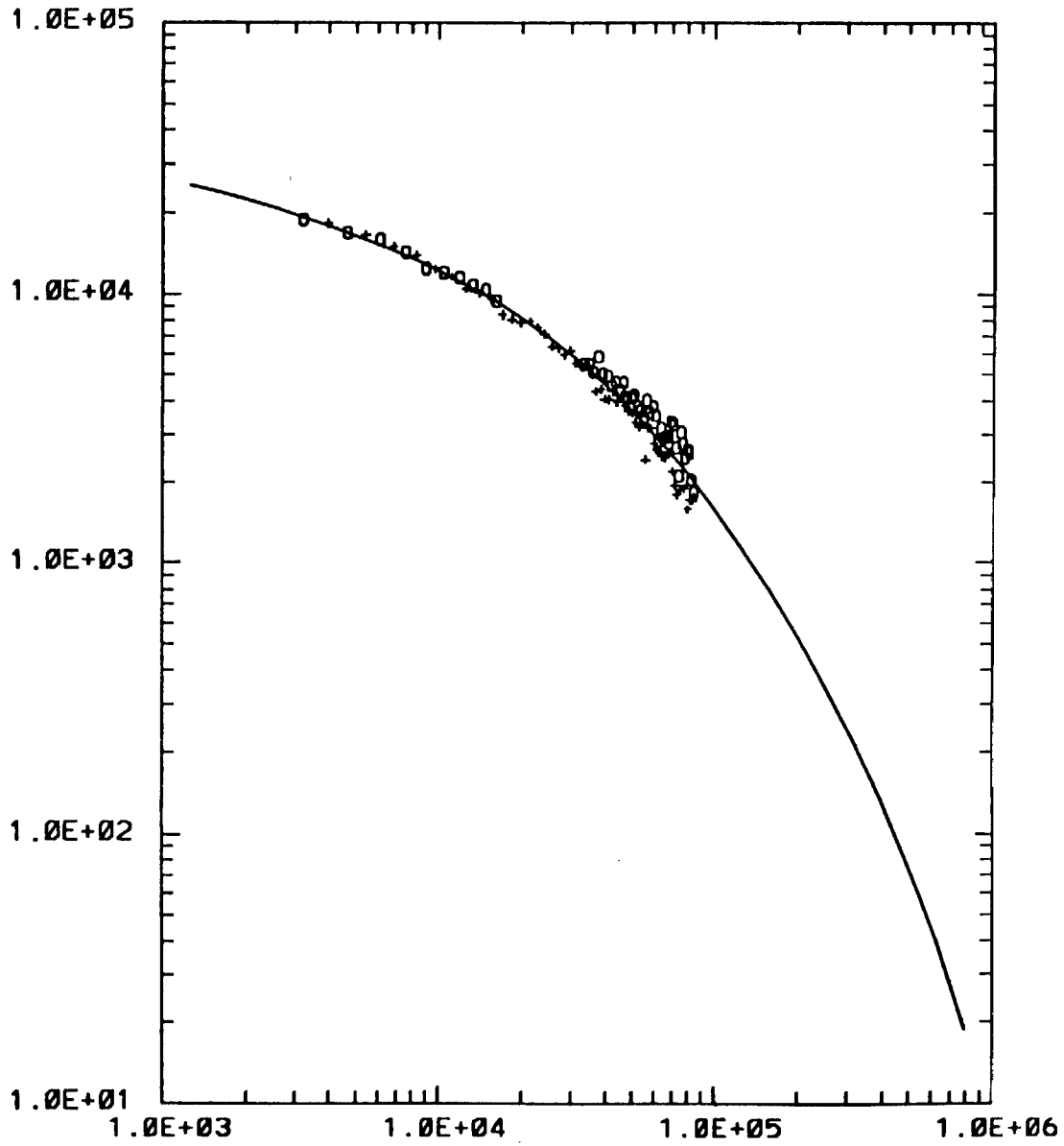
jancn1su.sd
1.0E+05
1.0E+04
1.0E+03
1.0E+02
1.0E+01
1.0E+03
1.0E+04
1.0E+05
1.0E+06
Scale Lengths = (2.512E+04 +/- 3.383E+03); (3.755E+05 +/- 1.576E+05)

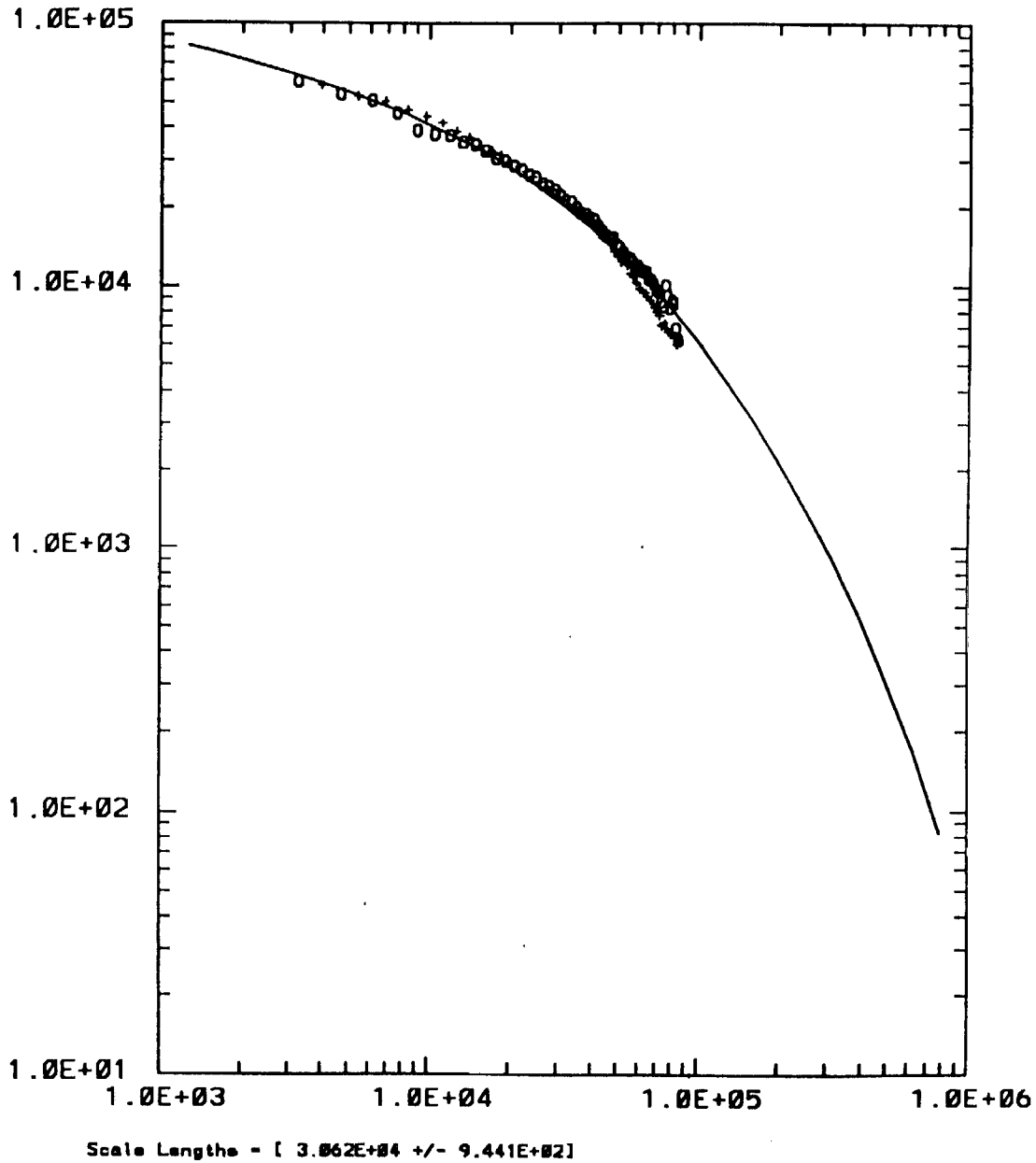
j11cn1cd.sd
1.0E+05
1.0E+04
1.0E+03
1.0E+02
1.0E+01
1.0E+03
1.0E+04
1.0E+05
1.0E+06
Scale Lengths = [3.862E+04 +/- 9.441E+02]

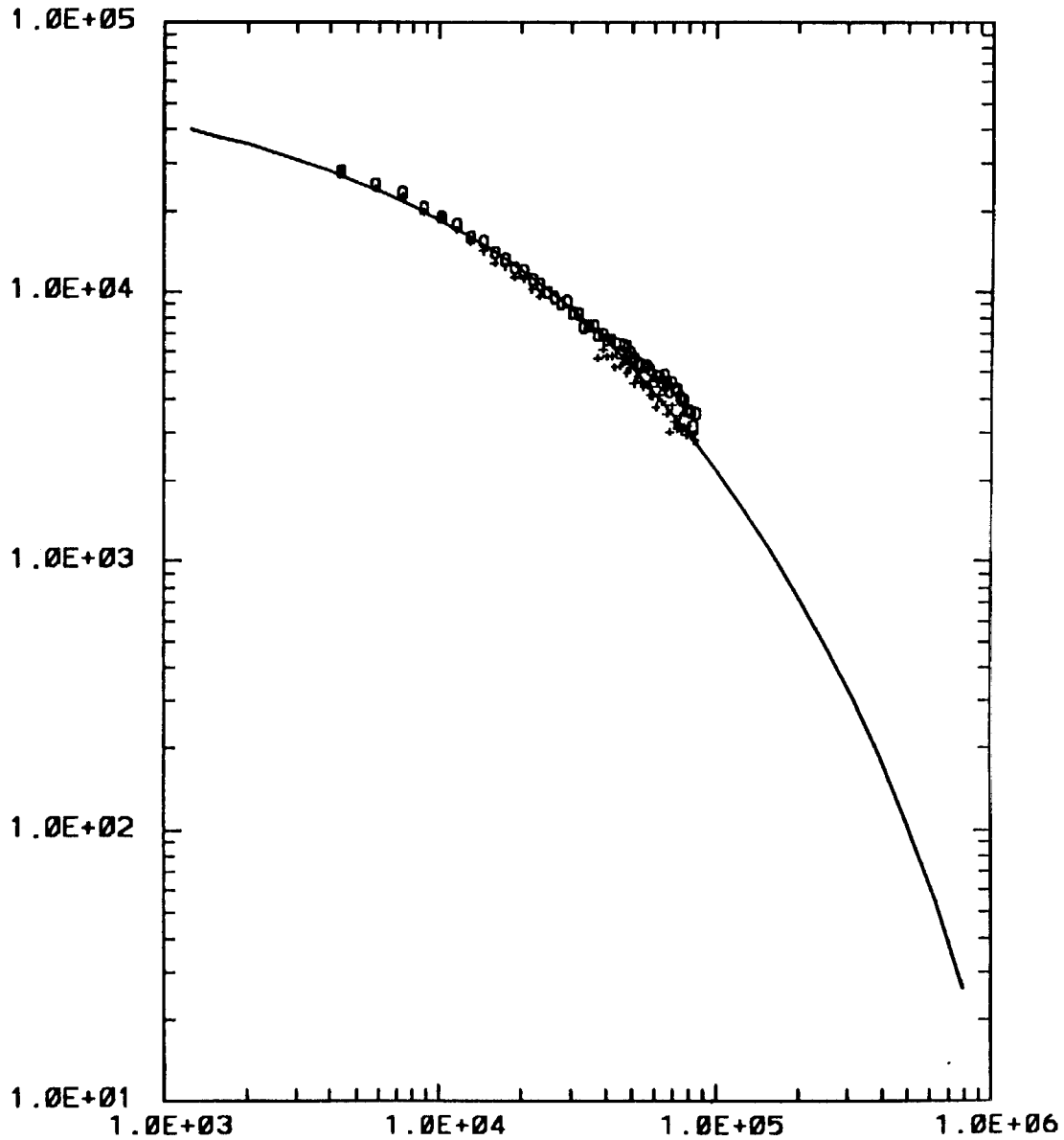
j12cn1su.sd
1.0E+05
1.0E+04
1.0E+03
1.0E+02
1.0E+01
1.0E+03
1.0E+04
1.0E+05
1.0E+06
Scale Lengths = [2.138E+04 +/- 7.435E+02]

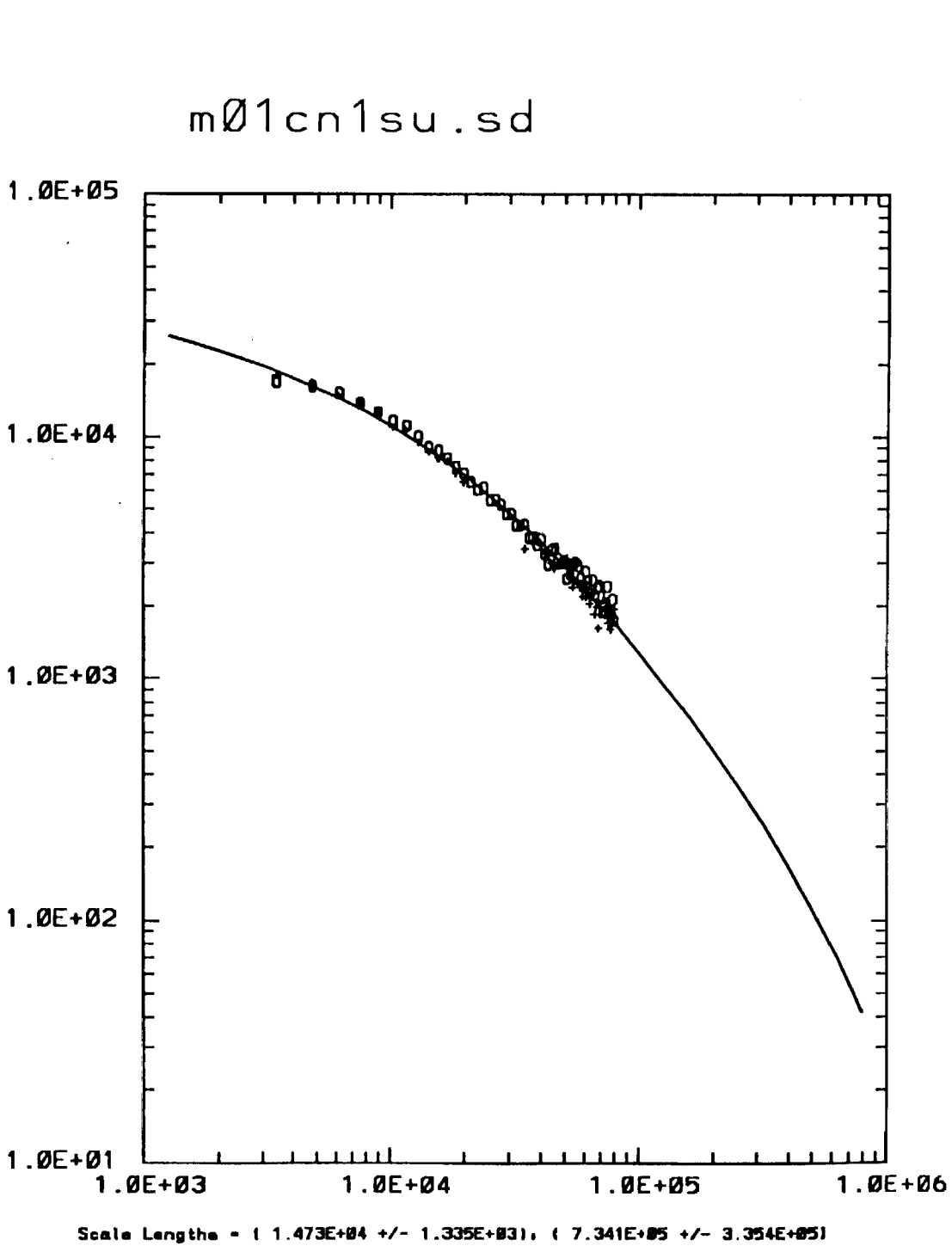
m01cn1su.sd
1.0E+05
1.0E+04
1.0E+03
1.0E+02
1.0E+01
1.0E+03
1.0E+04
1.0E+05
1.0E+06
Scale Lengths = (1.473E+04 +/- 1.335E+03), (7.341E+05 +/- 3.354E+05)

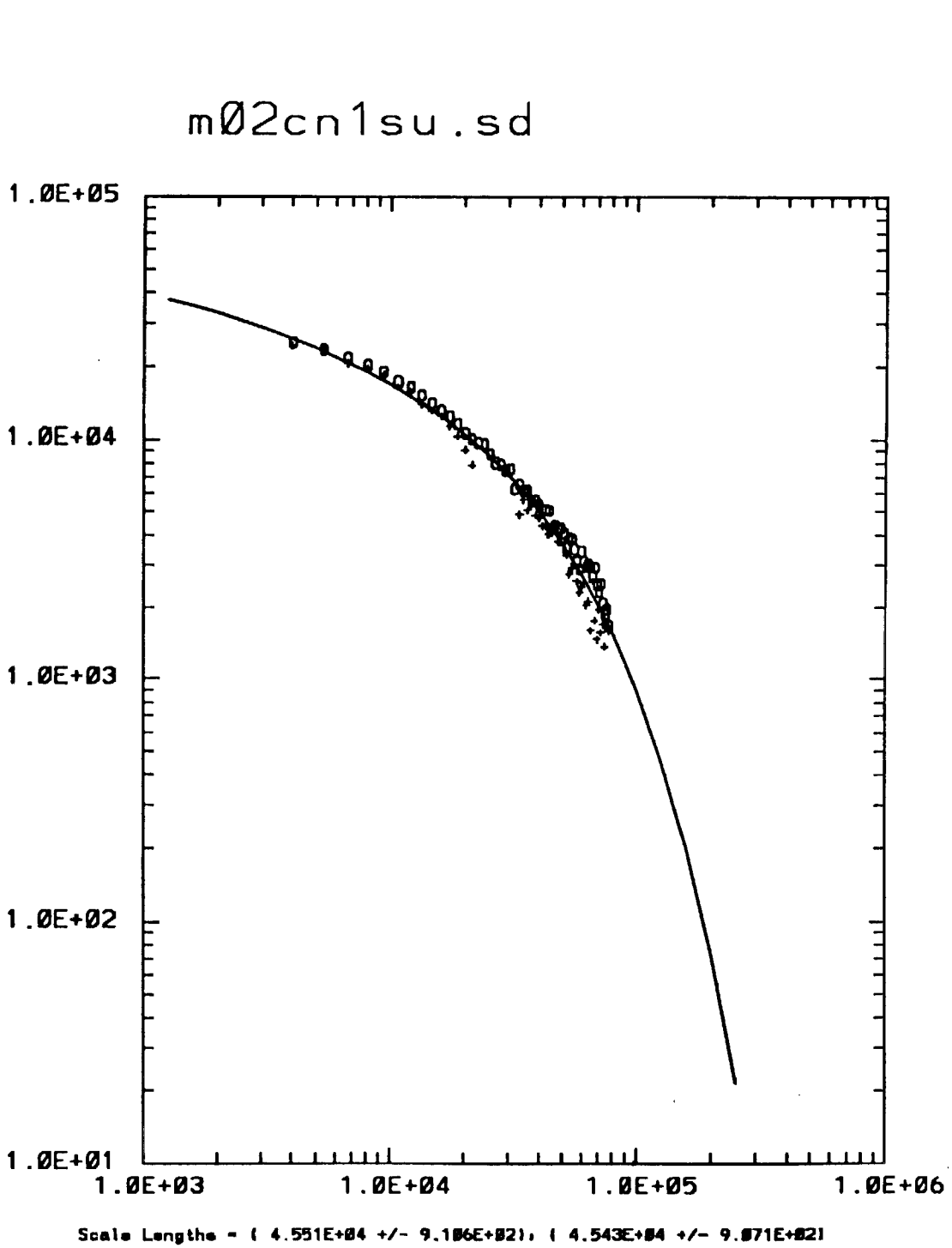
m02cn1su.sd
1.0E+05
1.0E+04
1.0E+03
1.0E+02
1.0E+01
1.0E+03
1.0E+04
1.0E+05
1.0E+06
Scale Lengths = (4.551E+04 +/- 9.186E+02), (4.543E+04 +/- 9.071E+02)

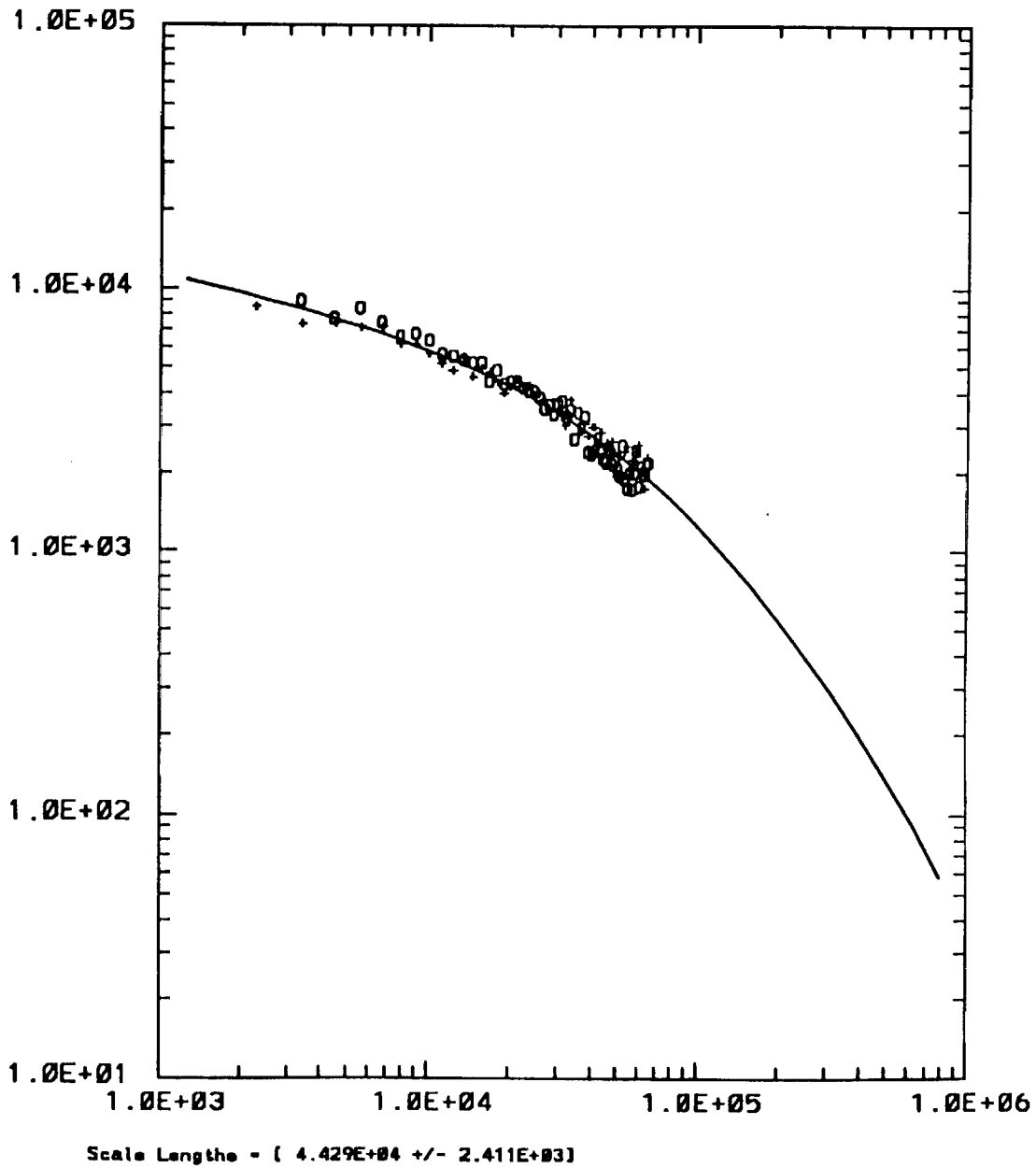
e86cn1su.sd
1.0E+05
1.0E+04
1.0E+03
1.0E+02
1.0E+01
1.0E+03
1.0E+04
1.0E+05
1.0E+06
Scale Lengths = [4.429E+04 +/- 2.411E+03]

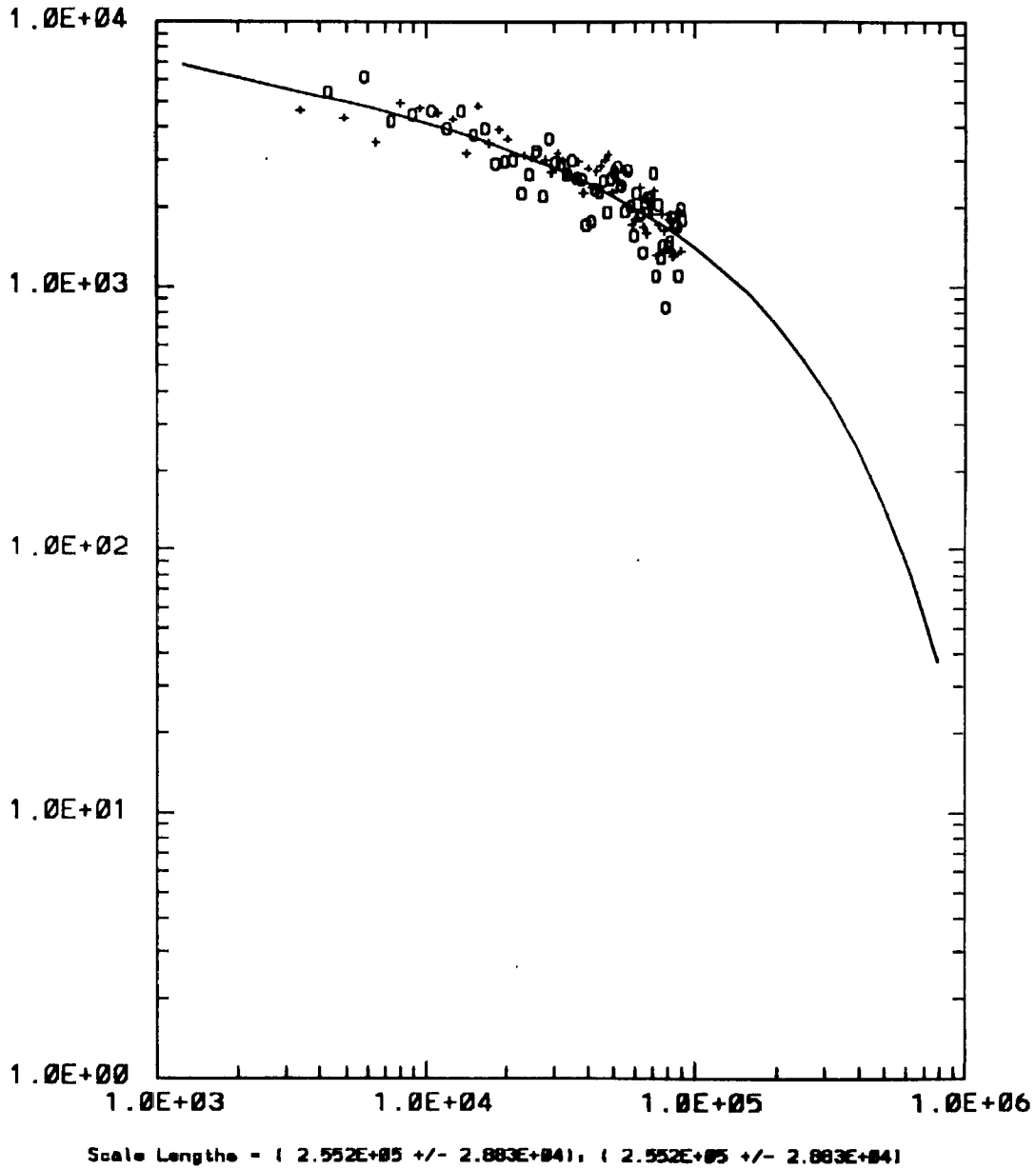
i85c2sum.sd
1.0E+04
1.0E+03
1.0E+02
1.0E+01
1.0E+00
1.0E+03
1.0E+04
1.0E+05
1.0E+06
Scale Lengths = (2.552E+05 +/- 2.883E+04), (2.552E+05 +/- 2.883E+04)

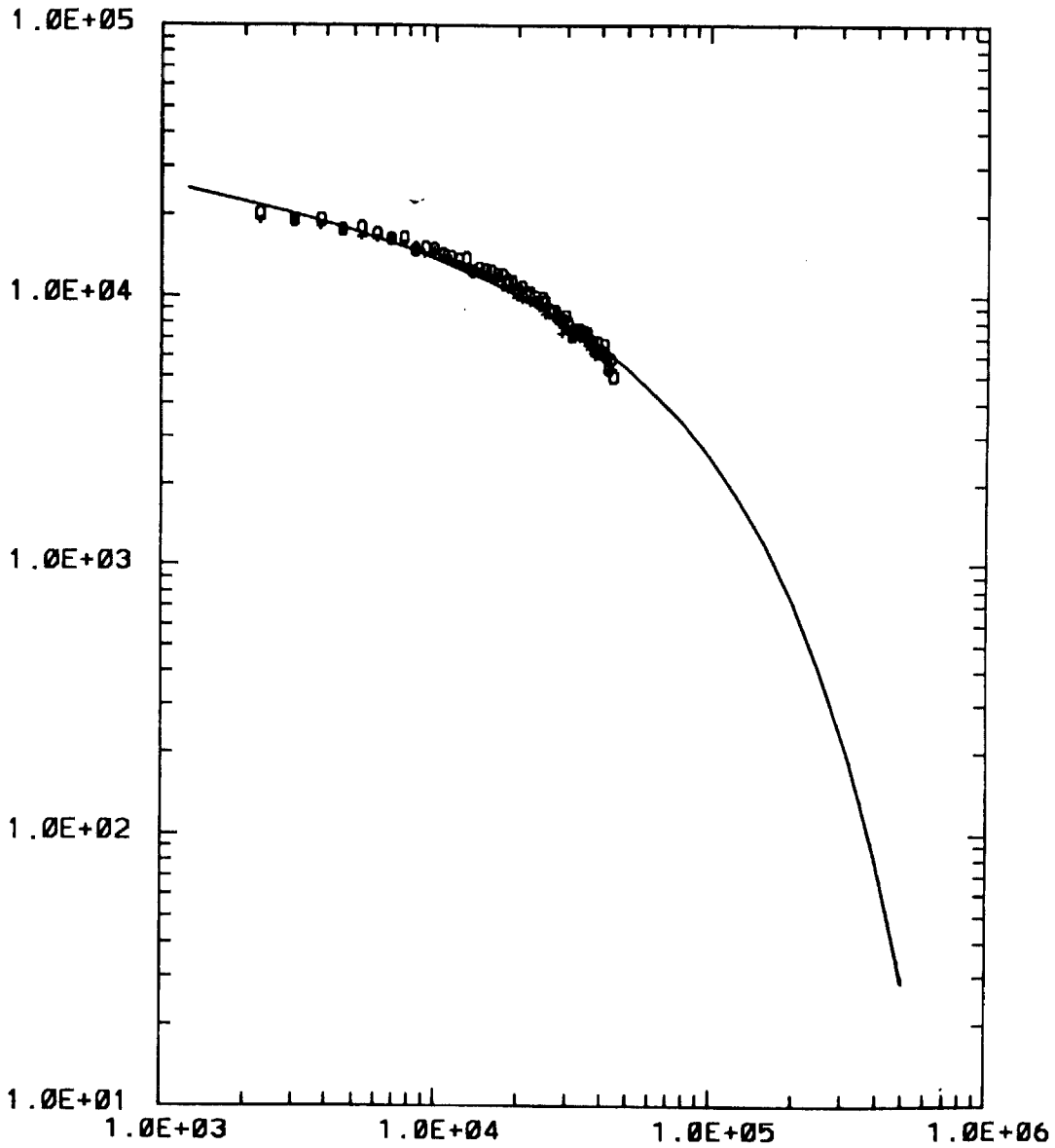
k190c2cd.sd
1.0E+05
1.0E+04
1.0E+03
1.0E+02
1.0E+01
1.0E+03
1.0E+04
1.0E+05
1.0E+06
Scale Lengths = (1.867E+05 +/- 3.912E+03), (1.867E+05 +/- 3.912E+03)

a174c2.sd

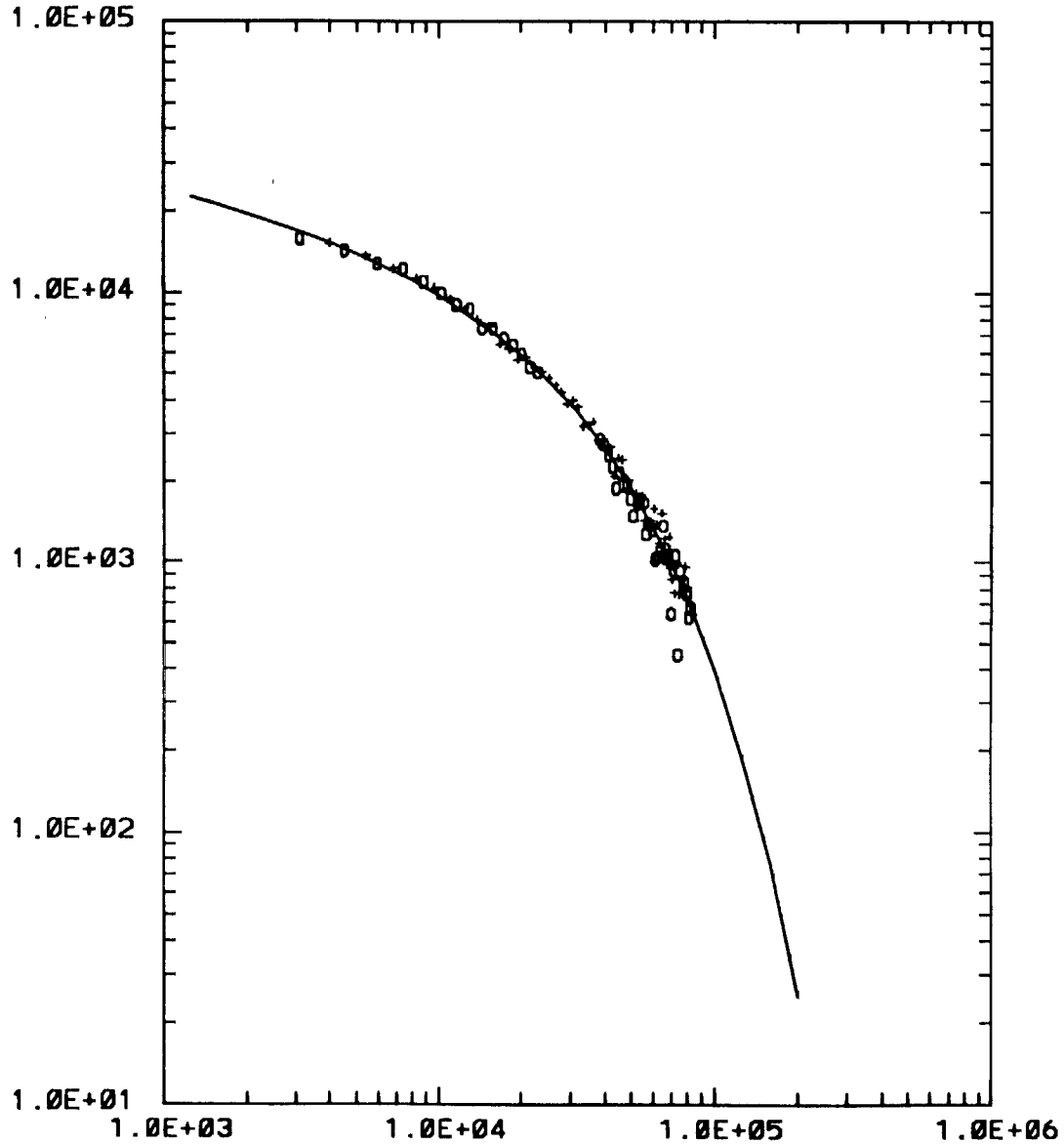

Scale Lengths = (4.843E+04 +/- 5.733E+02), (4.843E+04 +/- 5.733E+02)

janc2sum.sd

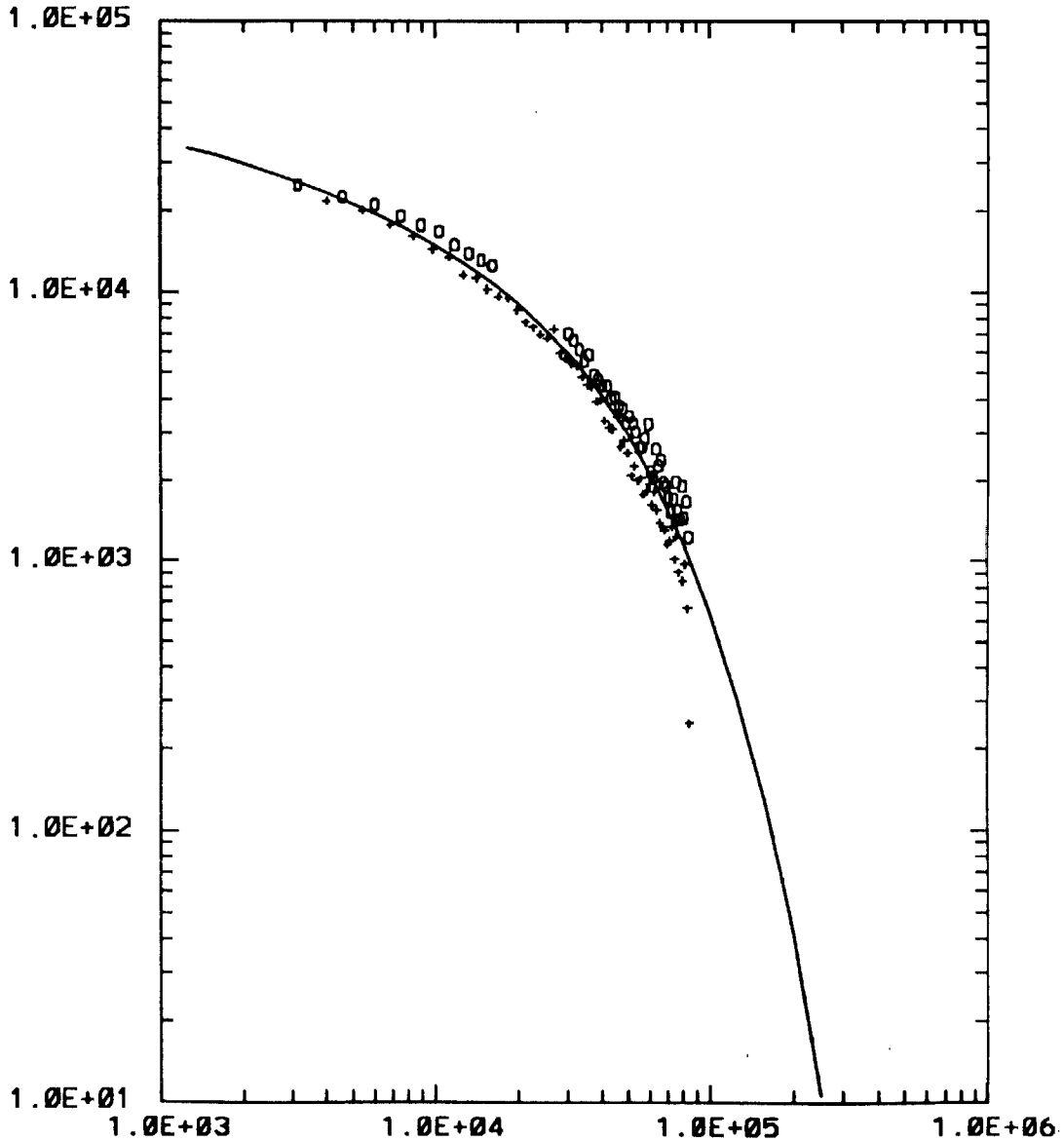

Scale Lengths = (4.119E+04 +/- 1.093E+03); (4.119E+04 +/- 1.093E+03)

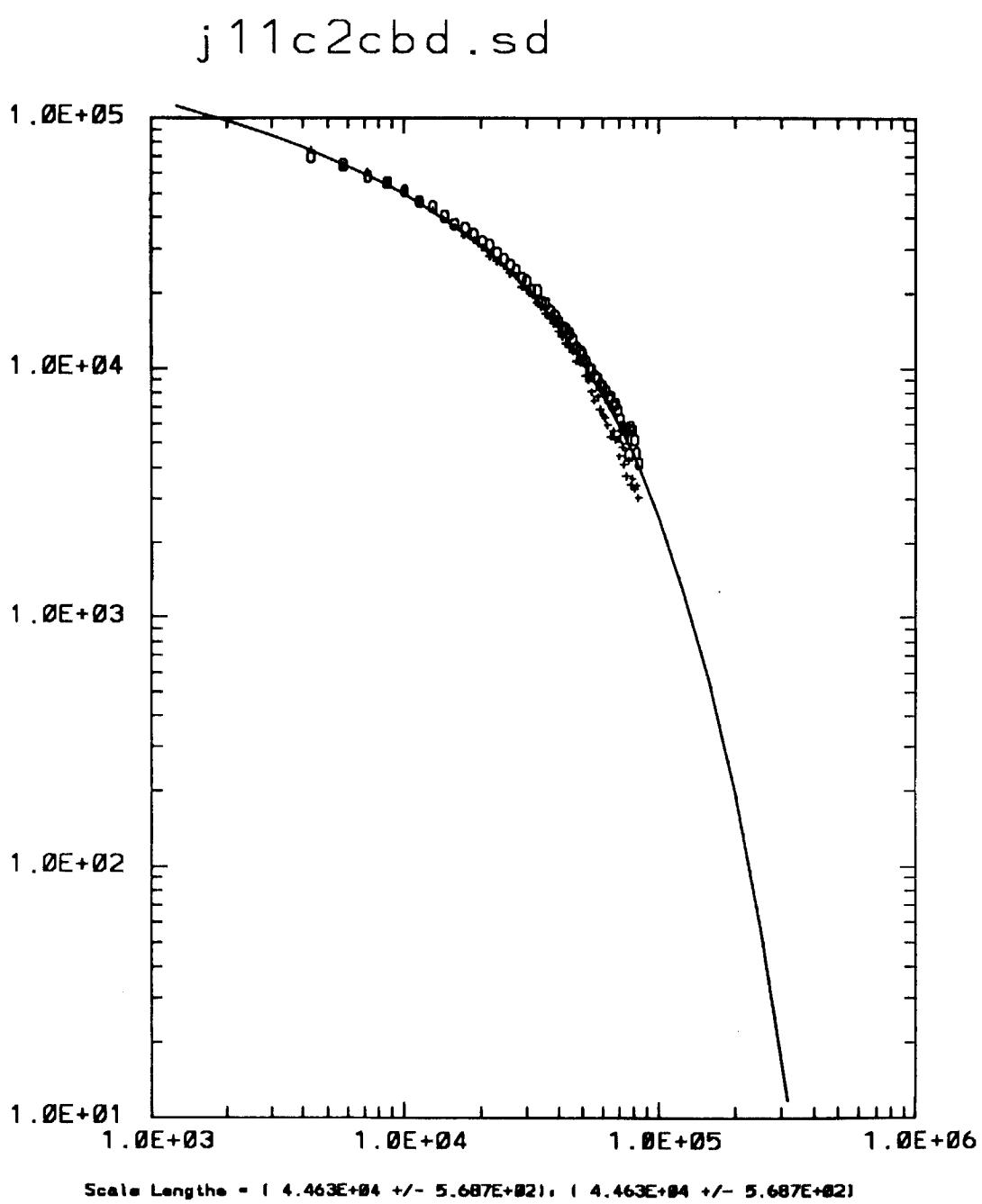
j11c2cbd.sd
1.0E+05
1.0E+04
1.0E+03
1.0E+02
1.0E+01
1.0E+03
1.0E+04
1.0E+05
1.0E+06
Scale Lengths = (4.463E+04 +/- 5.687E+02), (4.463E+04 +/- 5.687E+02)

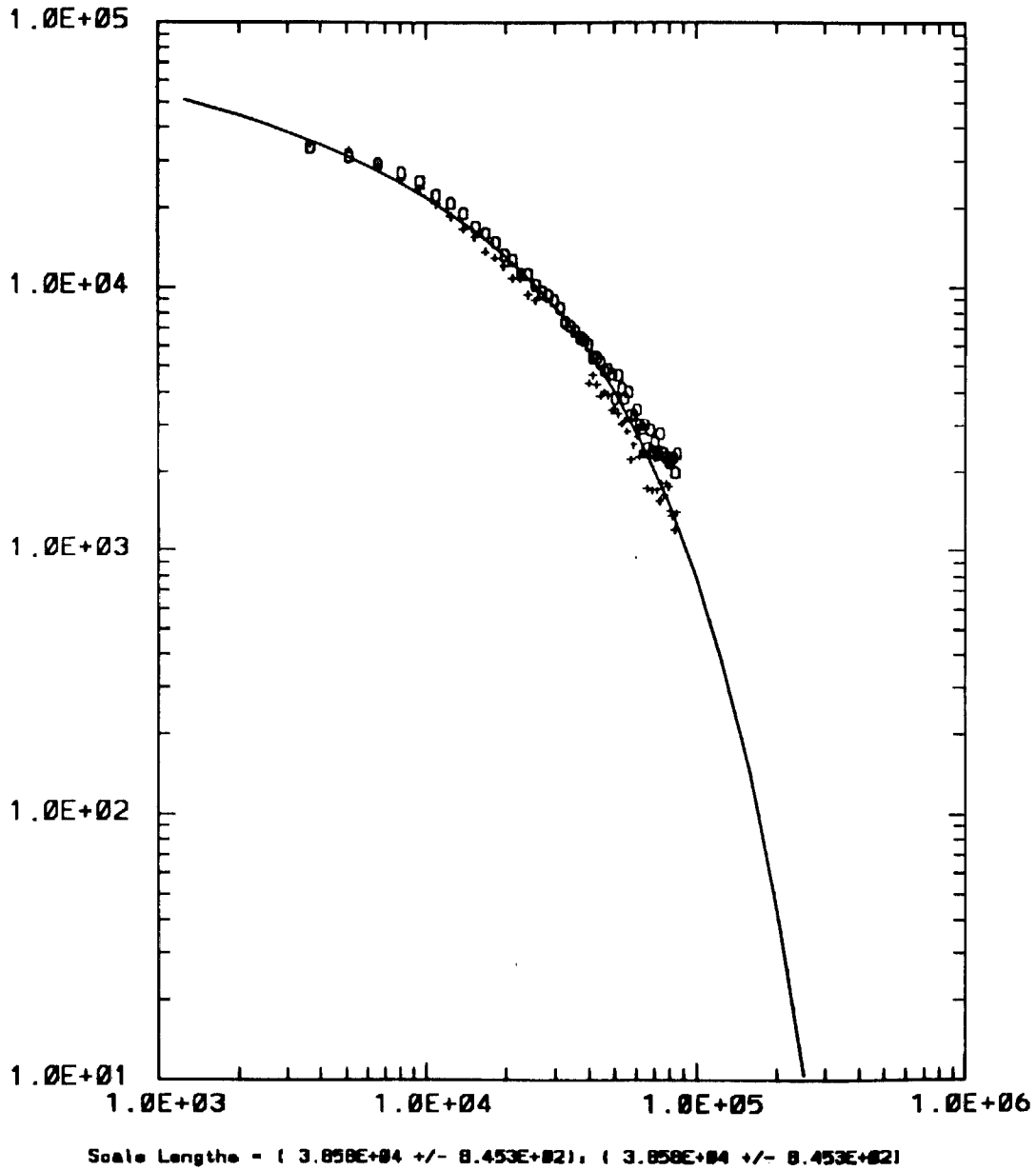
j12c2sum.sd
1.0E+05
1.0E+04
1.0E+03
1.0E+02
1.0E+01
1.0E+03
1.0E+04
1.0E+05
1.0E+06
Scale Lengths = (3.858E+04 +/- 8.453E+02), (3.858E+04 +/- 8.453E+02)

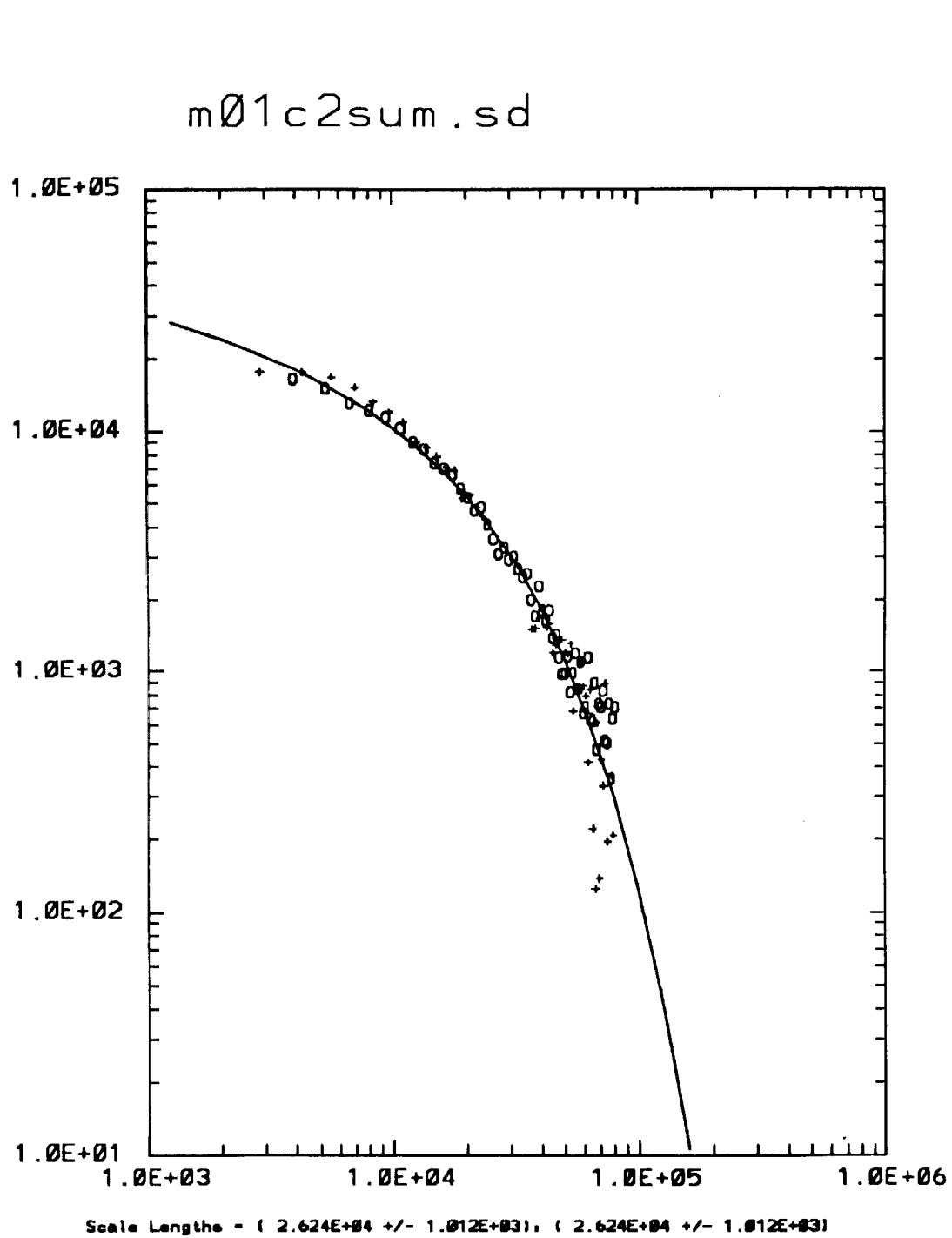
m01c2sum.sd
1.0E+05
1.0E+04
1.0E+03
1.0E+02
1.0E+01
1.0E+03
1.0E+04
1.0E+05
1.0E+06
Scale Lengths = (2.624E+04 +/- 1.012E+03); (2.624E+04 +/- 1.012E+03)

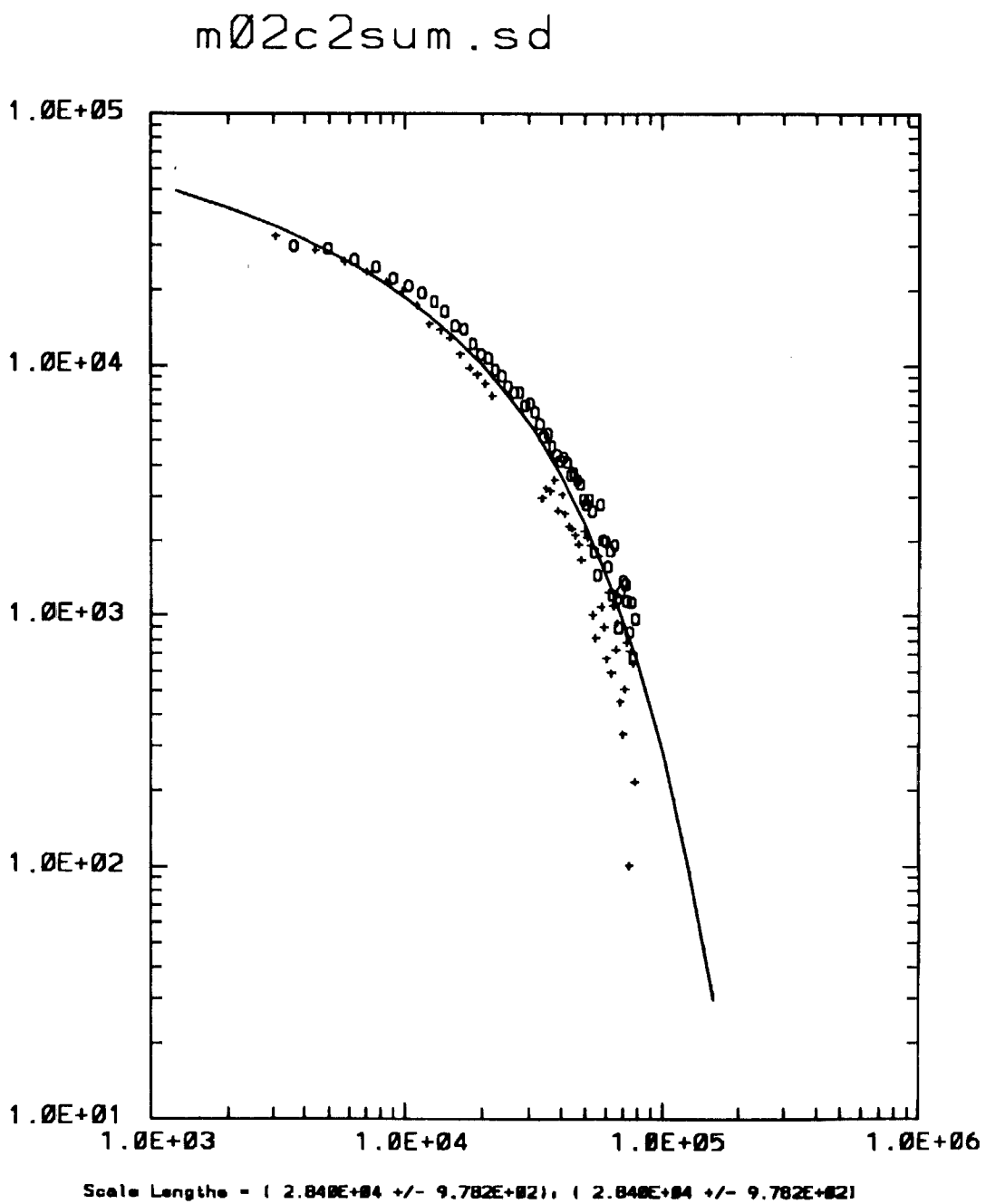
m02c2sum.sd
1.0E+05
1.0E+04
1.0E+03
1.0E+02
1.0E+01
1.0E+03
1.0E+04
1.0E+05
1.0E+06
Scale Lengths = (2.840E+04 +/- 9.782E+02), (2.840E+04 +/- 9.782E+02)

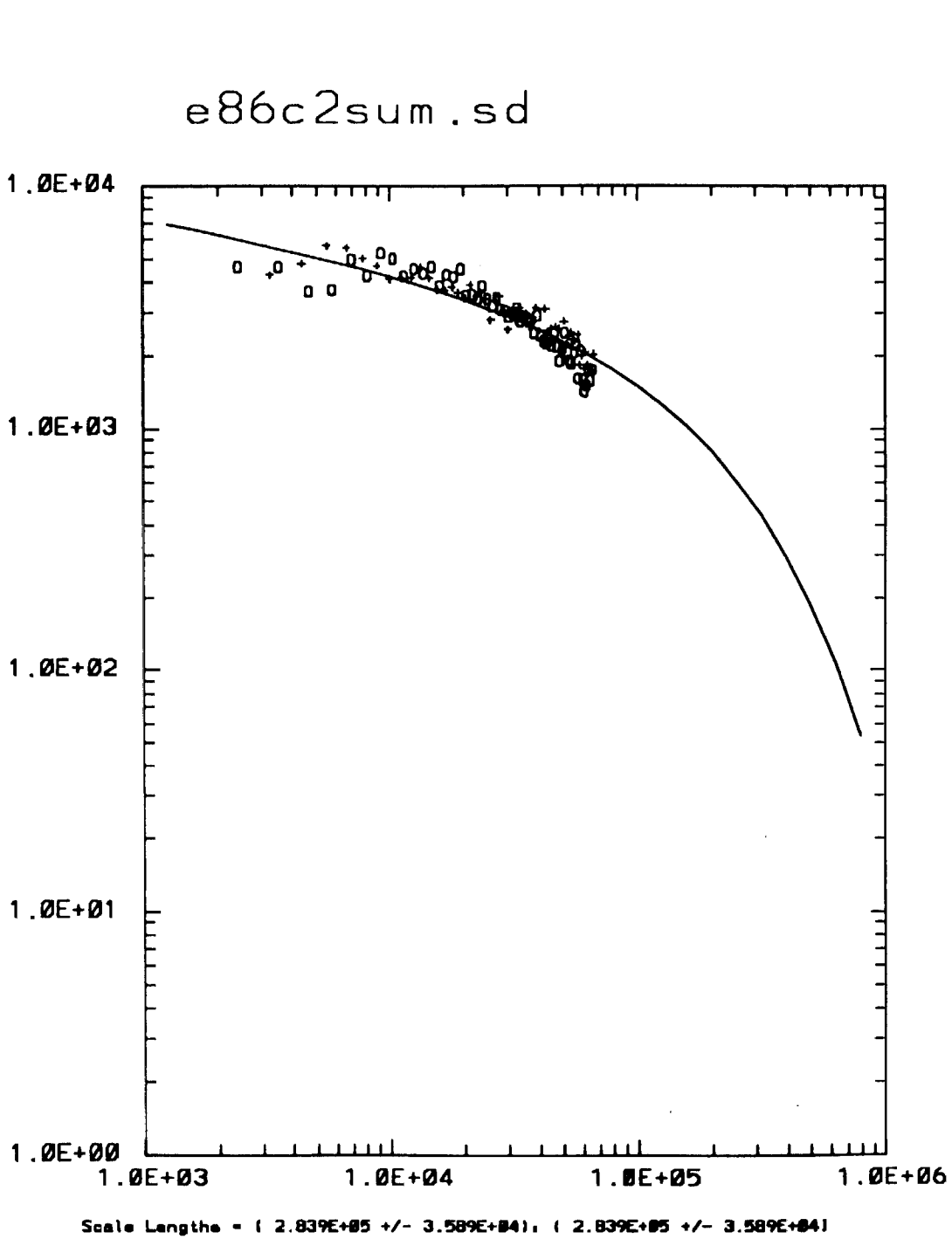
e86c2sum.sd
1.0E+04
1.0E+03
1.0E+02
1.0E+01
1.0E+00
1.0E+03
1.0E+04
1.0E+05
1.0E+06
Scale Lengths = (2.839E+05 +/- 3.589E+04), (2.839E+05 +/- 3.589E+04)